Pharmacological Research 87 (2014) 42–59

Contents lists available at ScienceDirect

Pharmacological Research

journal homepage: www.elsevier.com/locate/yphrs

Invited Review

ErbB/HER protein-tyrosine kinases: Structures and small molecule inhibitors

Robert Roskoski Jr.*

Blue Ridge Institute for Medical Research, 3754 Brevard Road, Suite 116, Box 19, Horse Shoe, NC 28742, USA

ARTICLE INFO

Article history:
Received 2 June 2014
Received in revised form 3 June 2014
Accepted 3 June 2014

Chemical compounds studied in this article:
Afatinib (PubMed CID: 10184653)
Canertinib (PubMed CID: 156413)
Dacomitinib (PubMed CID: 11511120)
Erlotinib (PubMed CID: 176870)
Gefitinib (PubMed CID: 123631)
Lapatinib (PubMed CID: 208908)
Neratinib (PubMed CID: 9915753)
Poziotinib (PubMed CID: 25127713)
Vandetinib (PubMed CID: 3081361)
WZ4002 (PubMed CID: 44607530)

Keywords:
Catalytic spine
EGFR
Gatekeeper residue
Regulatory spine
Targeted cancer therapy
Transition-state inhibitor

ABSTRACT

The epidermal growth factor receptor (EGFR) family consists of four members that belong to the ErbB lineage of proteins (ErbB1–4). These receptors consist of an extracellular domain, a single hydrophobic transmembrane segment, and an intracellular portion with a juxtamembrane segment, a protein kinase domain, and a carboxyterminal tail. The ErbB proteins function as homo and heterodimers. Growth factor binding to EGFR induces a large conformational change in the extracellular domain. Two ligand-EGFR complexes unite to form a back-to-back dimer in which the ligands are on opposite sides of the aggregate. Following ligand binding, EGFR intracellular kinase domains form an asymmetric dimer. The carboxyterminal lobe of the activator kinase of the dimer interacts with the amino-terminal lobe of the receiver kinase thereby leading to its allosteric stimulation. Several malignancies are associated with the mutation or increased expression of members of the ErbB family including lung, breast, stomach, colorectal, head and neck, and pancreatic carcinomas. Gefitinib, erlotinib, and afatinib are orally effective protein-kinase targeted quinazoline derivatives that are used in the treatment of *ERBB1*-mutant lung cancer and lapatinib is an orally effective quinazoline derivative used in the treatment of ErbB2-overexpressing breast cancer. Moreover, monoclonal antibodies that target the extracellular domain of ErbB2 are used for the treatment of ErbB2-positive breast cancer and monoclonal antibodies that target ErbB1 and are used for the treatment of colorectal cancer. Cancers treated with these targeted drugs eventually become resistant to them, and a current goal of research is to develop drugs that are effective against drug-resistant tumors.

Contents

Abbreviations: AL, activation loop; AMP-PNP, 5′-adenylyl-β, γ-imidodiphosphate; AS, activation segment; C-spine, catalytic spine; CDK, cyclin-dependent kinase; EC, extracellular; EGFR, epidermal growth factor receptor; FDA, United States Food and Drug Administration; 3-FPM, 3-fluorophenylmethoxy; NSCLC, non-small cell lung cancer; Nrg, neuregulin; JM, juxtamembrane; PK, protein kinase; R-spine, regulatory spine; TGFα, transforming growth factor α; TM, transmembrane; MW, molecular weight.

* Tel.: +1 828 891 5637; fax: +1 828 890 8130.
E-mail address: rrj@brimr.org

http://dx.doi.org/10.1016/j.phrs.2014.06.001
1043-6618/

1. Introduction to ErbB/HER

1.1. Biology of the ErbB/HER family of receptors

The ErbB/HER receptor protein-tyrosine kinases are ubiquitously expressed in epithelial, mesenchymal, cardiac, and neuronal cells and in their cellular progenitors [1]. This group of receptors, which includes the epidermal growth factor receptor (EGFR), is among the most studied cell signaling families in biology. They regulate apoptosis, cell cycle progression, differentiation, development, and transcription. EGFR was the first receptor to be characterized as a protein-tyrosine kinase, which was a revolutionary finding at the time (see Ref. [2] for a historical review). The human epidermal growth factor receptor family consists of four members (HER1–4) that belong to the ErbB lineage of proteins (ErbB1–4). The corresponding human gene synonyms include: (i) *EGFR/ERBB1/HER1*, (ii) *ERBB2/HER2/NEU*, (iii) *ERBB3/HER3*, and (iv) *ERBB4/HER4*.

Eleven polypeptide growth factor ligands, which are divided into four groups, interact with the ErbB receptors [3]. The first group consists of epidermal growth factor (EGF), epigen (EPG), transforming growth factor-α (TGFα), and amphiregulin (AR); group I ligands bind to EGFR. The second group consists of betacellulin (BTC), heparin-binding epidermal growth factor-like growth factor (HB-EGF), and epiregulin (EPR); group II ligands bind to EGFR and ErbB4. The third group consists of neuregulin-1 (Nrg-1) and neuregulin-2 (Nrg-2); group III ligands bind to ErbB3 and ErbB4. The fourth group consists of neuregulin-3 (Nrg-3) and neuregulin-4 (Nrg-4); group IV ligands bind to ErbB4. EGF contains 53 amino acid residues and the other factors are of similar size except for Nrg-1/2/3, which contain more than 200 residues. For comparison, human insulin contains 51 amino acid residues.

The human protein kinase family is one of the largest gene families consisting of more than 500 members [4]. These enzymes play a predominant regulatory role in nearly every aspect of cell biology. Protein kinases catalyze the following reaction:

$$ATP^{4-} + \text{protein—O : H} \rightarrow \text{Protein—O : } PO_3{}^{2-} + ADP^{3-} + H^+$$

Note that the phosphoryl group ($PO_3{}^{2-}$) and not the phosphate group ($OPO_3{}^{2-}$) is transferred to the protein substrate. A divalent cation such as Mg^{2+} facilitates the reaction. The activity of some protein kinases *in vitro* is greater with Mn^{2+} than Mg^{2+}, but the cellular concentration of the latter is greater than that of Mn^{2+}, and the physiological substrate is $MgATP^{1-}$. Serine and threonine contain an alcoholic side chain, and tyrosine contains a phenolic side chain. Based upon the nature of the phosphorylated —OH group (alcohol or phenol), these proteins are classified as protein-serine/threonine kinases (385 members), protein-tyrosine kinases (90 members), and tyrosine-kinase like proteins (44 members). Of the 90 protein-tyrosine kinases, 58 are receptor and 32 are non-receptor kinases. Protein phosphorylation is the most widespread class of post-translational modification used in signal transduction [4]. Families of protein phosphatases catalyze the dephosphorylation of proteins thus making phosphorylation–dephosphorylation an overall reversible process [5].

1.2. Protein kinases as drug targets

Besides their overall importance in signal transduction, protein kinases represent attractive drug targets [6]. Dysregulation of protein kinases occurs in a variety of diseases including cancer, diabetes, and autoimmune, cardiovascular, inflammatory, and nervous disorders. There are currently 250 or more protein kinase inhibitors in various stages of clinical development worldwide. Such drug discovery programs have led to the approval of about two dozen protein-kinase inhibitors by the FDA since 2003 (www.brimr.org/PKI/PKIs.htm). Nearly all of these approved drugs are used for the treatment of neoplastic disorders except for tofacitinib (pronounced "toe fa sye' ti nib"), which is used in the treatment of rheumatoid arthritis, an inflammatory disorder. See Ref. [7] for a description of reversible (types I, I ½, and II), irreversible, and allosteric protein kinase inhibitors.

Rask-Andersen et al. identified 145 protein kinases as the targets of currently approved or investigational drugs in clinical trials [8]. Of these, they report that 93 protein kinases are new targets and they represent about 20% of the 475 unique targets identified in clinical trials by these investigators. They report that G-protein coupled receptors represent the second highest class with 46 novel drug-targets.

Schechter et al. found that the *Neu* oncogene, which was induced in rats by ethylnitrosourea, is related to the rat *Erbb2* gene of the EGF receptor family [9]. This finding provided a clue on the potential role of the ErbB family of receptors in the pathogenesis of cancer. The ErbB family has undergone extensive study owing to its general role in signal transduction and in the pathogenesis of a variety of malignancies including lung, breast, stomach,

colorectal, head and neck, and pancreatic carcinomas [3]. The role of ErbB1 and ErbB2 in these malignancies has led to the development of three small molecule protein kinase inhibitors (afatinib, erlotinib, gefitinib) that target oncogenic *EGFR* mutants and are FDA-approved for the treatment of lung cancer and one (lapatinib) that targets ErbB2 and is approved in the treatment of breast cancer [3]. Panitumumab is a monoclonal antibody that inhibits EGFR and is approved for the treatment of colorectal cancer. Moreover, cetuximab inhibits EGFR and is approved for the treatment of colorectal and head and neck cancer. Additionally, pertuzumab targets ErbB2 and is approved for the treatment of metastatic breast cancer. Trastuzumab inhibits ErbB2 and is approved for the treatment of ErbB2-positive breast, gastric, and gastroesophageal cancers. Ado-trastuzumab emtansine is an antibody-drug conjugate that interacts with ErbB2 and is approved for the treatment of breast cancer [3].

2. Overview of ErbB/HER receptor structure and activation

2.1. Receptor homo and heterodimers

Ullrich et al. were the first to determine the amino acid sequence of a receptor protein-tyrosine kinase (EGFR) using cDNA sequence analysis [10]. They hypothesized that the receptor consisted of an extracellular domain, a single hydrophobic transmembrane segment, and an intracellular domain with protein kinase activity. This hypothesis has stood the test of time and fundamentally applies to all receptor protein kinases. The ErbB family of protein kinases consists of a glycosylated extracellular domain that is divided into four parts: domains I and III, which participate in ligand binding, and domains II and IV, which contain numerous cysteine residues that participate in disulfide bond formation [3]. Domain II participates in homo and heterodimer formation with ErbB family members. The extracellular domain is followed by a single transmembrane segment of 19–25 amino acid residues and an intracellular portion of about 540 amino acid residues that contains (i) a 40-residue juxtamembrane (JM) segment, (ii) a 270-residue protein kinase domain, and (iii) a 230-residue carboxyterminal tail.

There are two widely used numbering systems for the ErbB family amino acid residues [3]. The system used in the Uniprot knowledge base includes the signal peptide yielding numbers that correspond to the nascent receptor. The system employed by Ullrich et al. [10] and many others for ErbB1 excludes the 24-residue signal peptide and corresponds to the mature protein. Similarly, there are two numbering systems for the other family members, one of which corresponds to the nascent protein while the second excludes the signal peptide and corresponds to the mature protein. To parallel usage in specific papers, both systems are used in this review and care is taken to specify whether the nascent (plus signal peptide) or mature protein (minus signal peptide) residue numbers are employed.

Like all receptor protein-tyrosine kinases, the ErbB family functions as dimers or higher oligomers [1]. ErbB2 fails to bind to any growth factor so that physiological ErbB2 homodimer formation is unlikely. However, unphysiological overexpression of ErbB2 leads to the formation of a functional homodimer, which is important in the pathogenesis of many breast cancers [11]. ErbB3 is kinase impaired so that induced homodimer formation would fail to stimulate protein kinase activity and downstream signaling. However, kinase-impaired ErbB3 possesses 1/1000th of the autophosphorylation activity of ErbB1 [12] and the possibility exists that the ErbB3 homodimer is functional. ErbB2 is the favored dimerization partner for all of the other ErbB family members [13,14], and the ErbB2 heterodimer combinations with ErbB1 or ErbB3 exhibit robust signaling activity [15]. The heterodimer consisting of ErbB2, which lacks a ligand, and ErbB3, which is kinase impaired, is surprisingly the most robust signaling complex of the ErbB family [15].

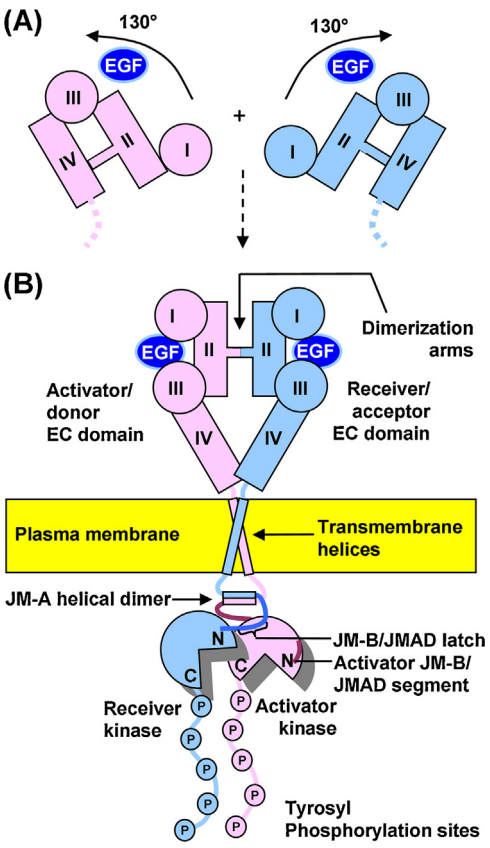

Fig. 1. Overview of the structure and dimerization mechanism of ErbB1. (A) Ligand binding to the extracellular domain of ErbB1 induces a large conformational shift in the extracellular domains. (B) Structure of the ErbB1 asymmetric dimer. The activator receptor is colored pink and the receiver is light blue. The carboxyterminal portion of the activator kinase domain interacts with the amino-terminal portion of the receiver kinase domain.

Source: The figure is modified from Ref. [19].

Binding of growth factors to ErbB1/3/4 promotes dimerization of monomeric receptors and increases the tyrosyl kinase activity of the intracellular domains of ErbB1/2/4 [16]. There are a number of possible ways that a growth factor or ligand can induce receptor dimerization. One possibility for growth-factor mediated receptor dimerization involves a single ligand that interacts simultaneously with two receptor molecules and effectively cross links them to form a dimeric complex [1]. Another possibility results when both ligands and both receptors contribute directly to the dimerization interface.

In contrast, the ErbB family employs a receptor-only mediated dimerization mechanism [1,17,18]. The activating ligand, EGF [17] or TGFα [18], contacts two distinct sites in domains I and III within a single EGFR molecule. Ligand binding promotes a large conformational change in the extracellular segment that opens the extracellular receptor domains and removes a β-hairpin–loop dimerization arm from a sleeve in domain IV (Fig. 1) [20]. Before the ligand binds, the arm is completely buried in domain IV, which stabilizes a closed or tethered receptor conformation that restricts its movement so that both ligand binding and dimerization are autoinhibited. Ligand binding breaks the intramolecular tether and allows the dimerization arm to enter a different sleeve in domain II of a

second ligand-bound receptor molecule, thereby leading to the formation of a back-to-back dimer with the ligands widely separated.

2.2. Asymmetric dimer formation and ErbB/HER activation

In the general mechanism for the activation of receptor protein-tyrosine kinases, activating ligands or growth factors bind to the ectodomains of two receptors and induce the formation of an activated dimerization state [1]. The juxtaposed cytoplasmic kinase domains catalyze the phosphorylation of tyrosine residues, usually in the activation segment, that leads to protein kinase activation. The kinase domains also catalyze the phosphorylation of additional tyrosine residues that create docking sites for adaptor proteins or enzymes that result in downstream signaling. This phosphorylation is accomplished in *trans*, *i.e.*, the first member of the dimer mediates the phosphorylation of the second and the second member mediates phosphorylation of the first. Activated ErbB receptors may also catalyze the phosphorylation of other molecules that result in downstream signaling.

EGFR was the first receptor tyrosyl kinase to be discovered [2]; however, its activation mechanism differs from that of other receptor kinases. Generally phosphorylation of one or more residues within the activation segment of protein kinases is required for activation [21] and phosphorylation of EGFR Tyr869 in the activation segment occurs [22], but this phosphorylation is not required for activation (residue number includes the signal peptide) [23]. Instead, Zhang et al. found that ligand-activated EGFR kinase domains form an asymmetric homodimer that resembles the heterodimer formed by CDK2 and cyclin A, its activating protein [24]. In the EGFR asymmetric homodimer, one kinase domain plays the role of cyclin (the activator/donor) and the other kinase domain plays the role of CDK (the receiver/acceptor). The intracellular JM-A domains of the activator and receiver form an anti-parallel helical dimer (Fig. 1). The JM-B domain of the receiver kinase forms a latch with the C-terminal domain of the activator kinase. Like other receptor kinases, the activated receiver kinase catalyzes the phosphorylation of tyrosine residues of the activator kinase, which then serve as docking sites for downstream signaling. A similar mechanism is responsible for the activation of the other homo and heterodimers of the ErbB family of enzymes.

The CDK/cyclin-like dimer interface of EGFR is formed by the αGH loop (between the αG and αH-helices) and the end of the αI-helix of the activator monomer and the N-terminal extension (residues 672–685), the αC-helix, and the β4/5-loop of the receiver monomer (Fig. 2) (residues excluding the signal peptide) [24]. As described later, the αGHI helices play an important role in the functioning of many protein kinases. The asymmetric dimer interface results in the burial of ≈2020 Å^2 of surface area [24]. The core of the asymmetric EGFR kinase domain dimer is dominated by interactions between (i) the αH-helix of the activator kinase (Met928, Val924, Ile917) and (ii) the N-terminus of the kinase domain (Leu680, Ala678, Pro675) and the αC-helix (Pro729, Leu736, and Asn732) of the receiver kinase [24].

2.3. Drugs that inhibit protein–protein interaction

The dimer interface represents a potential drug target that would prevent ErbB/HER protein kinase activation. The development of protein–protein interaction inhibitors is in its early stages [25]. Most disease-modifying proteins exert their functions through interactions with other proteins, and they lack obvious druggable pockets for small molecules. Although protein–protein interactions are essential for many aspects of cellular function and provide immense potential for drug development, targeting such

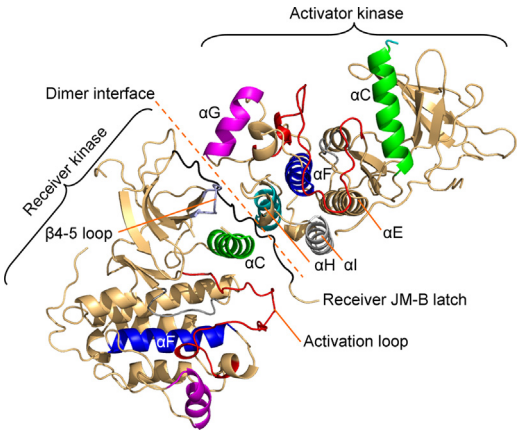

Fig. 2. Structure of the EGFR kinase domain asymmetric dimer. The dimeric interactions involve the receiver JM-B latch (black) and the αC-helix (green) of the amino-terminal lobe of the receiver kinase domain and the αG (magenta), αH (cyan), and αI (gray) portion of the carboxyterminal lobe of the activator kinase domain. As a result of these interactions, the receiver kinase is activated allosterically. The pdb coordinates were provided by Prof. John Kuriyan, and this figure and Figs. 3, 4, 6–9 and 12 were prepared using the PyMOL Molecular Graphics System Version 1.5.0.4 Schrödinger, LLC.

interactions with small molecules is challenging for two reasons. First, the contact surfaces between proteins usually involve a multitude of polar and hydrophobic interactions distributed across a large interface (a buried area of 1500–3000 Å^2). Unless an interaction hotspot can be identified, a drug with a small footprint is unable to bind with high affinity. Second, the protein–protein interfaces are usually flat. The lack of concavity limits the site of contact to only one side of a small molecule and such contacts have lower binding affinity than those involving multiple sites in a deeper cleft.

Small molecules potentially affect protein–protein interactions through at least three different mechanisms: orthosteric inhibition, allosteric inhibition, and interfacial binding/stabilization [25]. The first mechanism, orthosteric inhibition, involves direct competition with the interacting partners. These orthosteric inhibitors bind to the target proteins at sites that overlap with the regions that interact with the partner proteins, thus a protein–drug binary complex inhibits the formation of protein–protein complex. The second category comprises allosteric inhibitors. These small-molecule ligands bind to target proteins at sites distinct from the macromolecular interface. Ligand binding induces changes in the conformation of the target protein(s) and allosterically hinders macromolecular interactions. The third category contains interfacial binders, whereby the ligand and proteins form a ternary complex. An interfacial inhibitor binds to a pocket in the macromolecular interface and locks the complex into a nonproductive conformation.

Vemurafenib (PLX4032), which is an FDA-approved drug used in the treatment of B-Raf^{V600E}-positive melanomas [7], allosterically inhibits protein–protein interaction. A-Raf, B-Raf, and C-Raf are a family of three protein-serine/threonine kinases that participate in the Ras–Raf–MEK–ERK signal transduction cascade [26]. The formation of side-to-side Raf dimers is required for full kinase activity. Vemurafenib binds in the ATP pocket and displaces the regulatory αC-helix of B-Raf, which interferes with its dimerization with C-Raf and with B-Raf kinase activation [7,27]. The key residues comprising the dimer interface of B-Raf and C-Raf are outside of the ATP-binding pocket. Thus, vemurafenib allosterically inhibits Raf heterodimer formation and subsequent activation thereby accounting for its effectiveness in the treatment of melanomas. See Ref. [25] for a general discussion of protein–protein interaction inhibitors. Similar allosteric inhibition of EGFR protein–protein interaction by lapatinib is described in Section 6.4.

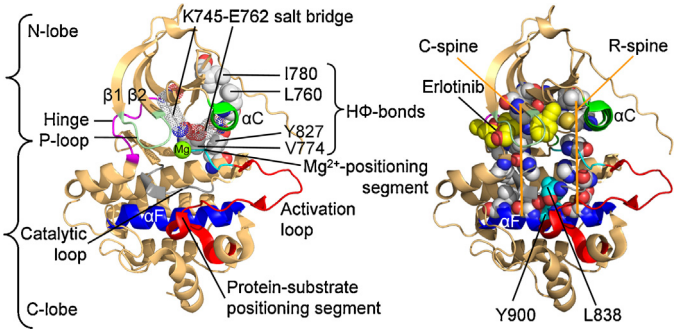

Fig. 3. (A) Overview of the structure of the active ErbB1 protein kinase domain complexed with erlotinib. The β3-lysine (K745) of the small N-lobe forms a salt bridge with αC-glutamate (E762); the residues are shown as sticks with surrounding dots. The activation segment of the large C-lobe is in an open conformation extending toward the right. The Mg^{2+}-positioning segment (cyan) consists of the first five and the substrate protein-positioning loop consists of the last eight residues of the activation segment. HΦ, hydrophobic. (B) Location of the R- and C-spines of ErbB1. The αF-helix forms the base of both the C- and R-spines. Leu838 of the catalytic loop forms a hydrophobic bond with Tyr900 of the αF-helix. These two residues are located between the hydrophobic R- and C-spines. The quinazoline group of erlotinib (yellow carbon atoms), which completes the catalytic spine, binds in approximately the same location as the adenine of ATP. The figures were prepared from PDB ID: 1M17 and 2ITN (for the superposition of the magnesium ion).

3. Overall structure of the ErbB/HER protein kinase domains

3.1. Properties of the small and large lobes

The ErbB/HER protein kinase domains have a small amino-terminal lobe and large carboxyterminal lobe first described by Knighton et al. for PKA (Fig. 3) [28]. The two lobes form a cleft that serves as a docking site for ATP. The small lobe contains a conserved glycine-rich (GxGxxG) ATP-phosphate-binding loop, sometimes called the P-loop, which is the most flexible part of the small lobe. This loop is near the phosphates of the ATP substrate. The β1 and β2-strands of the N-lobe harbor the adenine component of ATP and they interact with ATP-competitive small molecule inhibitors. The β3-strand typically contains an Ala–Xxx–Lys sequence, the lysine of which in EGFR (K645) forms a salt bridge with a conserved glutamate near the center of the αC-helix (E762) in protein kinases (nascent residues including the signal peptide). The presence of a salt bridge between the β3-lysine and the αC-glutamate is a prerequisite for the formation of the activate state and corresponds to the "αC-in" conformation. By contrast, Lys645 and Glu762 of the dormant form of EGFR fail to make contact and this structure corresponds to the displaced αC-out conformation. The αC-in conformation is necessary, but not sufficient, for the expression of full kinase activity.

The large lobe contains a mobile activation segment with an extended conformation in active enzymes and closed conformation in dormant enzymes. The first residues of the activation segment of protein kinases consist of DFG (Asp–Phe–Gly). The DFG exists in two different conformations. In the dormant activation segment conformation of many protein kinases including B-Raf [26], the aspartate side chain of the conserved DFG sequence faces away from the active site. This is called the "DFG-Asp out" conformation. In the active state, the aspartate side chain faces into the ATP-binding pocket and coordinates Mg^{2+}. This is called the "DFG-Asp in" conformation. This terminology is better than "DFG-in" and "DFG-out" because, in the inactive state, the DFG-phenylalanine may move into the active site while the DFG-aspartate moves out [29]; it is the ability of aspartate to bind (Asp-in) or not bind (Asp-out) to Mg^{2+} in the active site that is the key. However, the inactive conformations of the ErbB family kinases including kinase-impaired ErbB3 exist in the DGF-Asp in conformation. The Mg^{2+}-positioning loop of the ErbB protein kinases consists of the first five residues of the activation segment (DFGLA) (Fig. 3).

The activation segment of protein kinases typically ends with APE (Ala–Pro–Glu), but is ALE (Ala–Leu–Glu) in the ErbB family. The last eight residues of the activation segment in the ErbB family include PIKWMALE, which make up the protein-substrate positioning loop. The R-group of proline in this sequence serves as a platform that interacts with the tyrosyl residue of the peptide/protein substrate that is phosphorylated [30]. In protein-serine/threonine kinases, the serine or threonine interacts with backbone residues near the end of the activation segment and not with an R-group. Although the activation segment of the ErbB family contains a phosphorylatable tyrosine, in contrast to most other protein-tyrosine kinases [31], its phosphorylation is not required for enzyme activation [23,32].

Two conserved hydrophobic bonds in protein kinases and EGFR contribute to kinase domain stability. A hydrophobic bond between Leu760, which is two residues N-terminal to the Glu762 in the αC-helix, with Ile780 near the N-terminus of the β-4 strand helps to stabilize the N-terminal lobe. Moreover, another hydrophobic bond from Val774 in the αC-β4 loop of the small lobe and Tyr827 near the carboxyterminal end of the αE-helix in the large lobe (about eight residues upstream from HRD of the catalytic loop) further stabilizes the interaction between the two lobes (Fig. 3).

3.2. Secondary structure of the ErbB/HER protein kinase domains: the protein kinase fold

The small lobe of all protein kinases is dominated by a five-stranded antiparallel β-sheet (β1–β5) and the important regulatory αC-helix (Fig. 4) [33]. The first X-ray structure of a protein kinase (PKA, 1CPK) [28] depicted an αA and an αB-helix proximal to αC, but these first two helices are not conserved in the protein kinase family. ErbB1/2/4 are functional protein kinases that occur in similar active and variable inactive conformations. In contrast, ErbB3 is kinase impaired and lacks essential catalytic residues as noted later. Its X-ray structure is that of an inactive protein kinase. Although it possesses all of the α-helices and most of the β-sheets observed in all protein kinases, the αC-helix of ErbB3 is notably short (Fig. 4E).

The large lobe of the ErbB family of protein kinases is mainly α-helical with six conserved segments (αD–αI) that occur in all protein kinases [33] (Fig. 4). The first X-ray structure of a protein kinase (PKA) possessed a short helix proximal to the αF-helix, which was not named. However, this αEF helix is conserved in all protein kinase structures and represents a seventh-conserved segment in the C-lobe. The αF helix forms an important hydrophobic core. The large lobe of active ErbB1/2/4 contains a helix between the αH and αI segment (αHI) (Fig. 4B). The initial portion of the activation segment of inactive ErbB3 contains an αAL-helix that abuts against the αC-helix that favors its inactive displaced conformation (Fig. 4D). The dormant enzyme forms of ErbB1/2/4 also contain this helix in the proximal portion of the activation segment. The activation segment of active EGFR is open and extends outward while that of dormant ErbB3 is closed, more compact, and interferes with protein substrate binding (Fig. 4A and D).

The large lobe of active protein kinases contains four short β-strands (β6–β9) (Fig. 4A and B). The β6-strand, the primary sequence of which occurs before the catalytic loop (Fig. 5), interacts with the activation segment β9-strand. The β7-strand interacts with the β8-strand, the primary structures of which occur between the catalytic loop and the activation segment. The active forms of ErbB1/2/4 contain two additional β-strands (β10 and β11). The inactive forms of all four ErbB family members contain the β7- and

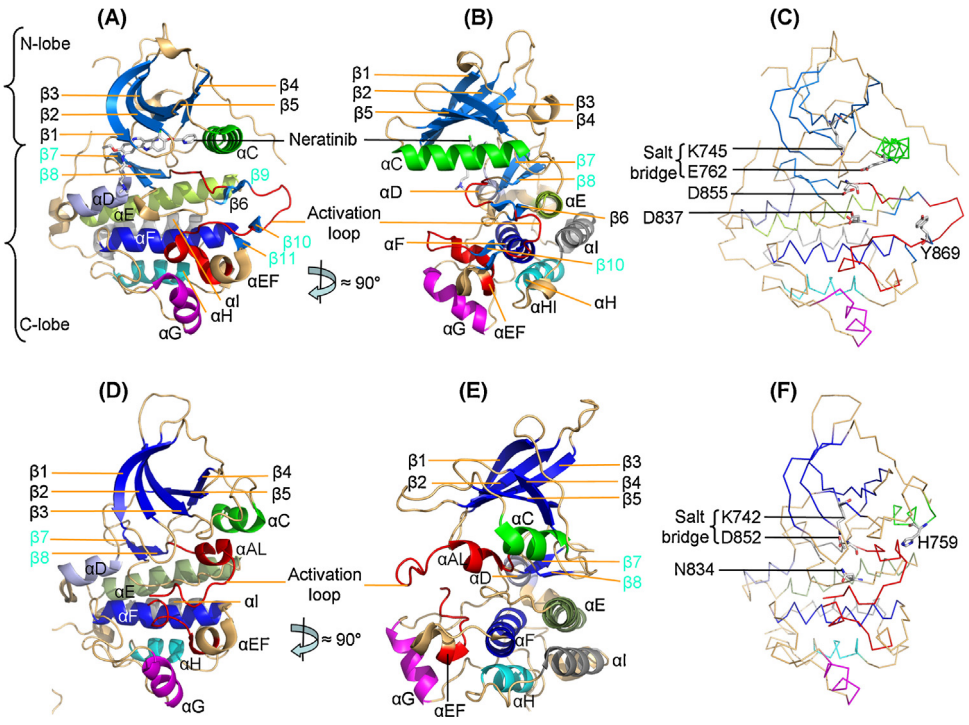

Fig. 4. Secondary structures of ErbB1 (PDB ID 3W2Q) and ErbB3 (PDB ID 3KEX). (A and B) Labeling of the ErbB1 α-helices and β-sheets. αC–I, αEF, and β1–9 are conserved secondary structures found in nearly all active protein kinase domains. (C) A salt bridge occurs between β4-Lys745 and αC-Glu762 in active ErbB1 (same view as (A)). D837 is the D of HRD; D855 is the D of DFG; Y869 is the phosphorylatable tyrosine in the activation segment. (D and E) Labeling of the ErbB3 α-helices and β-sheets. (F) A salt bridge occurs between β4-Lys742 and DFG-Asp852 in inactive ErbB3 (same view as (D)). In kinase-impaired ErbB3, H759 substitutes for glutamate in the α-C helix and N834 substitutes for aspartate in the catalytic loop HRD. Neratinib is an irreversible inhibitor that forms a covalent bond with Cys797 of ErbB1 or Cys805 of ErbB2. Owing to the bulky side chain of the anilinoquinoline scaffold, the drug binds to the displaced αC conformation. A portion of the activation segment in (D–F) is missing owing to its disorder in the X-ray structure. αAL, activation loop α-helix in dormant ErbB3.

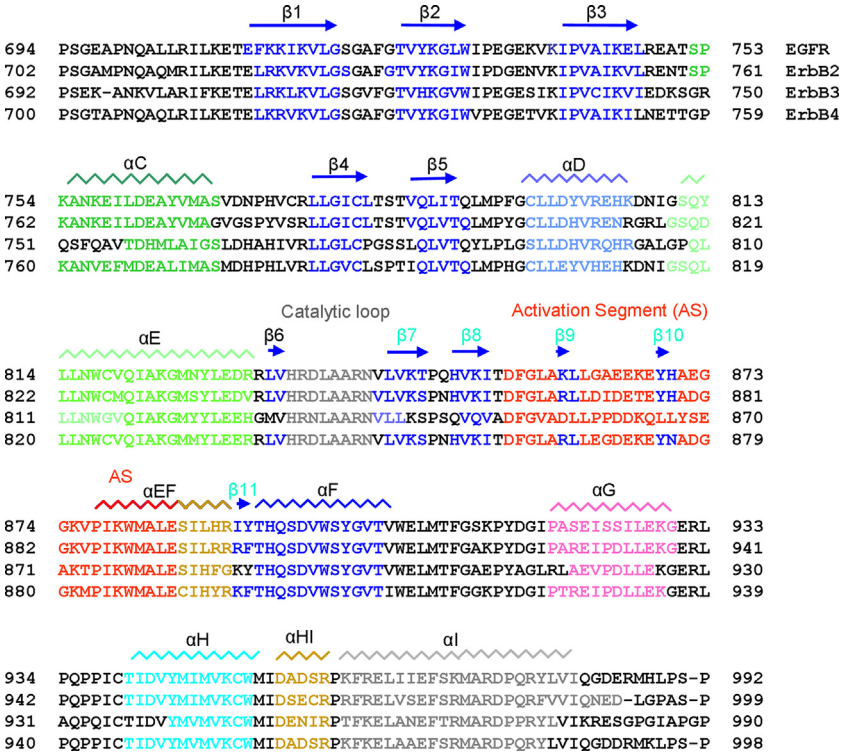

Fig. 5. Primary structure of the protein kinase domains of the ErbB family. The color code corresponds to that of Fig. 4. The zigzag lines correspond to α-helices and the arrows correspond to β-strands for active (ErbB1/2/4) and inactive (ErbB3) conformations. AS, activation segment.

β8-strands, but they all lack the β6- and β9- and the β10- and β11-strands.

There are two general kinds of conformational motions associated with all protein kinases including those of the ErbB family; one involves conversion of an inactive conformation into a catalytically competent form. Activation typically involves changes in the orientation of the αC-helix in the small lobe and the activation segment in the large lobe. The interconversion of the inactive and active forms of the ErbB kinases also involves an electrostatic switch. In the dormant enzymes, the β4-lysine (K742) forms a salt bridge with the DFG-Asp (D852) residue, as indicated for ErbB3 in Fig. 4F. The conversion to the active enzyme form entails an electrostatic switch where the β4-lysine (K745) forms a salt bridge with the αC-Glu (E762) with the concomitant formation of the αC-in conformation, as depicted for EGFR in Fig. 4C. The active forms of the ErbB1/4 possess the β4-lysine–αC-glutamate salt bridge (*e.g.*, PDB ID 1M41 for EGFR and 3BCE for ErbB4) and all of the dormant ErbB1–4 enzyme forms posses the β4-lysine–DFG-aspartate salt bridge (*e.g.*, PDB ID 4HJ0 for EGFR, 3RCD for ErbB2, 3KEX for ErbB3, and 3BBW for ErbB4) (for EGFR, see Supplemental movie 1).

Supplementary material related to this article can be found, in the online version, at http://dx.doi.org/10.1016/j.phrs.2014.06.001.

The active kinase then toggles between open and closed conformations as it goes through the catalytic cycle. The open form of the active enzyme binds MgATP and the protein substrate; this is accompanied by the conversion to the closed form as catalysis occurs. After catalysis, phosphorylated protein and then MgADP are released as the enzyme is reconverted to the open form prior to the next catalytic cycle.

3.3. Structures of the hydrophobic spines in the active and in the dormant ErbB/HER protein kinase domains

3.3.1. The regulatory spine

Taylor and Kornev [31] and Kornev et al. [34] analyzed the structures of active and dormant conformations of some two dozen protein kinases and determined functionally important residues by a local spatial pattern (LSP) alignment algorithm. In contrast to the protein kinase amino acid signatures such as DFG or HRD, the residues that constitute the spines were not identified by sequence analyses *per se*. Rather, they were identified by their three-dimensional location based upon a comparison of the X-ray crystallographic structures [31,34].

The local spatial pattern alignment analysis revealed a skeleton of four non-consecutive hydrophobic residues that constitute a regulatory or R-spine and eight hydrophobic residues that constitute a catalytic or C-spine (Fig. 3B). Each spine consists of residues derived from both the small and large lobes. The regulatory spine contains residues from the activation segment and the αC-helix, whose conformations are important in defining active and dormant states. The catalytic spine governs catalysis by facilitating ATP binding. The two spines dictate the positioning of the protein substrate (R-spine) and ATP (C-spine) so that catalysis results. The proper alignment of the spines is necessary for the assembly of an active kinase.

ErbB1, ErbB2, and ErbB4 have been observed in both active (PDB ID: 1M14, 3PP0, 3BCE) and inactive (PDB ID: 4HJ0, 3RCD, 3BBW) conformations by X-ray crystallography. The authors who studied ErbB2 (PDB ID: 3PP0) in complex with an inhibitor described it as an "active-like enzyme" [35]; however, the β-4 lysine and the αC-glutamate fail to form a salt bridge so that this enzyme lacks the characteristics of a fully active protein kinase (the β-4 Lys743 binds to Asp863 of the DFG-aspartate). The X-ray structure of the kinase-impaired ErbB3 is observed only in an inactive conformation with the enzyme exhibiting the displaced αC-helix and a closed activation loop (PDB ID: 3KEX). The X-ray crystal structures of active EGFR, ErbB2, and ErbB4 are superimposable (α-carbon root mean square deviation < 1 Å). The inactive conformations of these the four ErbB family enzymes are also superimposable. However, the αC-helices and the activation segments of the active and inactive enzyme forms differ from one another (root mean square deviation > 6 Å).

The EGFR regulatory spine consists of a residue from the beginning of the β4-strand (Leu777, nascent protein residue numbers are used in this section), from the C-terminal end of the αC-helix (Met766), the phenylalanine of the activation segment DFG (Phe856), along with the HRD-histidine (His835) of the catalytic loop. Met766 and comparable residues from other protein kinases are four residues C-terminal to the conserved αC-glutamate. The backbone of His835 is anchored to the αF-helix by a hydrogen bond to a conserved aspartate residue (Asp872). The protein-substrate positioning loop, the activation loop, and the αHI loop of protein kinase domains, including the ErbB/HER family, bind to the αF-helix by hydrophobic bonds [31].

3.3.2. The catalytic spine

The catalytic spine of protein kinases consists of residues from the small and large lobes and is completed by the adenine base of ATP [31,34]. The two residues of the small lobe of the EGFR protein kinase domain that bind to the adenine group of ATP include Val726 from the beginning of the β2-strand and Ala743 from the conserved Ala–Xxx–Lys of the β3-strand. Furthermore, Leu844 from the middle of the β7-strand binds to the adenine base in the active enzyme. Val726, Ala743, and Leu844 characteristically form hydrophobic bonds with the scaffolds of ATP-competitive small molecule inhibitors. Val843 and Val845, hydrophobic residues that flank Leu844, bind to Leu798 at the beginning of the αD-helix. The αD-helix Leu798 binds to Thr903 and Leu907 in the αF-helix. Note that both the R-spine and C-spine are anchored to the αF-helix, which is a very hydrophobic component of the enzyme that is entirely within the protein and not exposed to the solvent. The αF-helix serves as a sacrum that supports the spines, which in turn anchor the protein kinase catalytic muscle. Table 1 lists the residues of the spines of human ErbB1–4 and the catalytic subunit of murine PKA.

3.3.3. The gatekeeper and other shell residues

Using site-directed mutagenesis, Western blotting, and sensitive radioisotopic enzyme assays, Meharena et al. identified three residues in PKA that stabilize the R-spine, and they referred to them as shell residues [36]. Going from the connecting aspartate in the αF-helix up to the spine residue in the β4-strand at the top, these investigators labeled the regulatory spine residues RS0, RS1, RS2, RS3, and RS4 (Fig. 6A and Table 1). The three shell residues are labeled Sh1, Sh2, and Sh3. Sh1 interacts with RS3 and Sh2. Sh2, which is the classical gatekeeper residue, interacts with Sh1 below it and with RS4 next to it. The term gatekeeper refers to the role of such residues in allowing or disallowing access to a hydrophobic back pocket adjacent to the adenine binding site [37,38] that is occupied by portions of many small molecule inhibitors as described in Section 6.4. Sh3 interacts with RS4. Using the previous local spatial pattern alignment data, only three of 14 amino acid residues in PKA surrounding RS3 and RS4 are conserved, and these are the shell residues that serve as collateral spinal ligaments that stabilize the protein kinase vertebral column or spine. The V104G mutation (Sh1) decreased the catalytic activity of PKA by 95%. The M120G (Sh2) and M118G (Sh3) double mutant was devoid of catalytic activity. These results provide evidence for the importance of the shell residues in maintaining protein kinase activity.

A comparison of the active and dormant EGFR R-spines shows that RS2, RS3, and RS4 of dormant EGFR are displaced when compared with active EGFR, a result that is consistent with the displaced

Table 1
ErbB1–4 and murine PKA residues that form the R-spine, R-shell, and C-spine.[a]

		ErbB1	ErbB2	ErbB3	ErbB4	PKA[b]
Regulatory spine						
β4-Strand (N-lobe)	RS4	Leu777	Leu785	Leu774	Leu783	Leu106
C-helix (N-lobe)	RS3	Met766	Met774	Ile763	Met772	Leu95
Activation loop (C-lobe) F of DFG	RS2	Phe856	Phe864	Phe853	Phe862	Phe185
Catalytic loop His or Tyr (C-lobe)[c]	RS1	His835	His843	His832	His841	Tyr164
F-helix (C-lobe)	RS0	Asp896	Asp904	Asp893	Asp902	Asp220
R-shell						
−2 residues from the gatekeeper	Sh3	L788	L796	L785	L794	M118
Gatekeeper, end of β4-strand	Sh2	T790	T798	T787	T796	M120
αC-β4 loop	Sh1	C775	S783	V772	V781	V104
Catalytic spine						
β2-Strand (N-lobe)		Val726	Val734	Val723	Val732	Val57
β3-A/CXK motif (N-lobe)		Ala743	Ala751	Cys740	Ala749	Ala70
β7-Strand (C-lobe)		Leu844	Leu852	Leu841	Leu850	Leu173
β7-Strand (C-lobe)		Val843	Val851	Val840	Val849	Leu172
β7-Strand (C-lobe)		Val845	Val853	Val842	Val851	Ile174
D-Helix (C-lobe)		Leu798	Leu806	Leu795	Leu804	Met128
F-Helix (C-lobe)		Thr903	Thr911	Thr900	Thr909	Leu227
F-Helix (C-lobe)		Leu907	Leu915	Leu904	Leu913	Met231

[a] Nascent residues including the signal peptide.
[b] From Ref. [31].
[c] Part of the HRD (His–Arg–Asp) or YRD (Tyr–Arg–Asp) sequence.

αC-helix configuration of the dormant enzyme (Fig. 6B, C and E). The RS3 and RS4 α-carbon atoms differ in location by 1.5 Å and 2.1 Å, respectively, and the *p*-carbon atoms of the phenyl ring of RS2 differ in location by 5.2 Å. The Sh1 residues of active and dormant EGFR are nearly superimposable while the α-carbon atoms of Sh2 and Sh3 are modestly displaced (1.1 and 1.8 Å, respectively) (Fig. 6E). The shell residues of EGFR and ErbB3 also vary in position. With the exception of Ala743 and Val726, the C-spines of active and dormant EGFR are nearly superimposable (see Supplemental movie 2). Furthermore, the residues of the C-spine that occur in active and dormant EGFR and in dormant ErbB3 are superimposable. Since the R-spine of active and inactive enzyme forms differ in structure, it is natural to expect that the surrounding shell residues will also vary in their three-dimensional location.

Supplementary material related to this article can be found, in the online version, at http://dx.doi.org/10.1016/j.phrs.2014.06.001.

3.4. Anchoring the activation segments of ErbB1/2/4 to the kinase domain

The phosphorylation of one or more residues in the activation segment of the majority of protein kinases is required to generate their active conformation. In the case of PKA, this corresponds to the phosphorylation of the activation loop Thr197 as catalyzed by PDK1 or PKA [39,40]. This activation loop phosphate interacts with four different sections of PKA including (i) His87 of the αC-helix, (ii) Arg165 of the catalytic loop H/YRD, (iii) Tyr215 in the αEF/αF loop, and (iv) Lys189 and Thr195 within the activation segment [34]. The glutamate at the end of the activation segment forms a conserved salt bridge with Arg280 in the αHI loop. Within the R-spine, Phe185 of DFG within the PKA activation segment forms hydrophobic bonds with Leu95 of the αC-helix and with Tyr164 of the catalytic loop (equivalent to the histidine HRD of most protein kinases).

Because phosphorylation is not required for activation of the ErbB protein kinases, other mechanisms must exist for stabilizing the active conformation of the activation loop and anchoring it to other portions of the kinase domain. The DFG-Phe856 (nascent EGFR residues) interacts with Met766 of the N-lobe αC-helix and the HRD-His835 of the C-lobe catalytic loop as part of the R-spine. Glu884 at the end of the activation segment forms a salt bridge with Arg958 that lies in the αHI loop. The activation segment β9-strand interacts with the β6-strand near the catalytic loop. These interactions parallel those of PKA. The activation segment β10-strand interacts with the β11-strand just proximal to the αF-helix; this interaction is lacking in PKA (Fig. 7). These β6- and β9-strand and β10- and β11-strand interactions are absent in the inactive conformations of ErbB1–4. The ErbB family activation segments contain

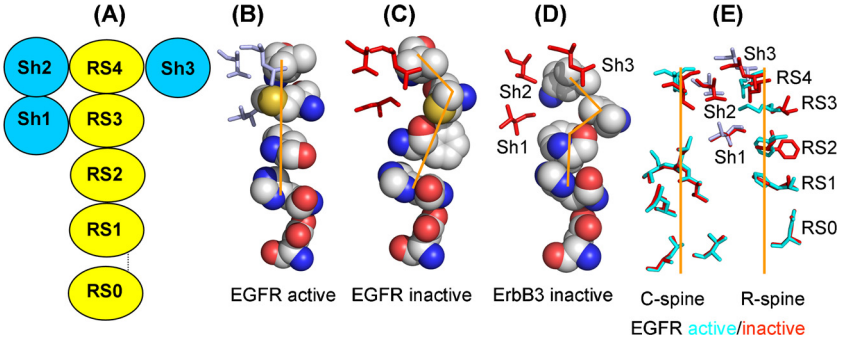

Fig. 6. Structure of ErbB catalytic and regulatory spines. (A) R-spine (RS) and R-shell (Sh) nomenclature and interaction partners. Sh2 represents the important gatekeeper residue found at the end of the β5-strand in the N-terminal lobe. (B) R-spine and shell residues of active EGFR (PDB ID: 1M14). (C) R-spine and shell residues of inactive EGFR (PDB ID: 4HJO). (D) R-spine and shell residues of inactive ErbB3 (PDB ID: 3KEX). (E) Superposition of the C-spines, shell residues and R-spines of active and inactive (red sticks) EGFR.

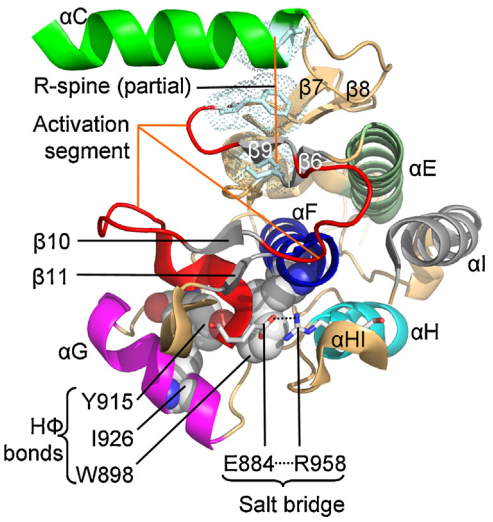

Fig. 7. Role of the R-spine, the β6–9 and β10–11 strands, and the salt bridge between the activation segment (Glu884) and the αHI loop (Arg958) in anchoring the activation segment to the EGFR kinase domain. Hydrophobic (HΦ) interactions comparable to those involving the αF-helix W898, the αFG-loop Y915, and the αG-helix I926 (nascent residue numbers) occur in most protein kinase domains. The figure was prepared from PDB ID: 1M14.

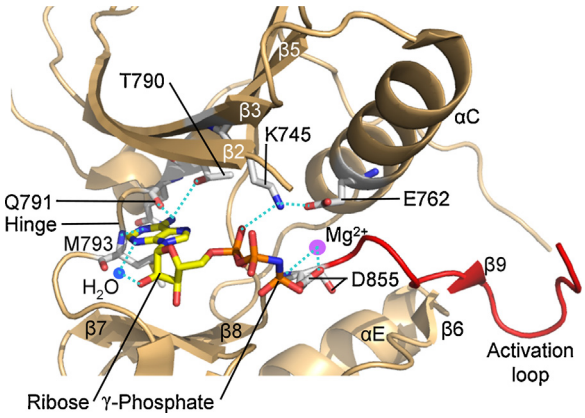

Fig. 8. ATP-binding site of the active Gly719Ser mutant of EGFR. The ATP analog, AMP-PNP, and selected residues that make polar contacts (cyan dashes) with it are shown as sticks. T790 is the gatekeeper residue, and Q791 and M793 are part of the hinge. The polar contacts extending from Mg^{2+} and D855 (the D of DFG) toward ATP interact with oxygen on the γ-phosphate, which is hidden in this view. The β-1 strand and P-loop are omitted for clarity. The figure was prepared from PDB ID: 2ITN.

four acidic glutamate residues (excluding the terminal glutamate of ALE) that might mimic negatively charged phosphate in stabilizing the activation segment. However, the X-ray crystal structures of the active forms of ErbB1/2/4 show that these four glutamates are directed toward the solvent and do not interact with the kinase domain.

Hydrophobic bonds occur within the activation segment involving (i) Phe856 (the Phe of DFG) and Leu 858 and (ii) Val876, Ile878, and Met881. However, these hydrophobic bonds occur in (i) both active (PDB ID: 1M14, 3PP0, 3BCE) and inactive ErbB1/2/4 (PDB ID: 4HJ0, 3RCD, 3BBW) and (ii) inactive ErbB3 (PDB ID: 3KEX); accordingly they fail to explain the stabilization of the activation segment in its functional conformation. Whether the β6–β9 and β10–β11 strands contribute significantly in anchoring the activation segment to the other portions of the kinase domain or whether other interactions are important is unclear. However, the stabilization of the ErbB family activation segment differs substantially from that observed in PKA.

4. Conserved catalytic and structural residues in the ErbB/HER protein kinase domains

4.1. Binding pocket for ATP and small molecule inhibitors

The glycine-rich loop, or P-loop, occurs universally in protein kinases and consists of a canonical GxGxxΦG sequence where Φ refers to a hydrophobic residue. This sequence in the ErbB family is composed of GSGAFG (Table 2). The P-loop, which forms a lid above the ATP phosphates, is characteristically one of the most mobile portions of the protein kinase domain. This mobility may be due to the requirement that the enzyme binds ATP and then releases ADP following catalysis. In PKA, the second glycine of the P-loop helps to anchor the α-phosphate and the third glycine anchors the β-phosphate of ATP [41]. These glycine residues in EGFR are close to the phosphates of ATP, but they do not form polar contacts with it (PDB ID: 2GS7). Additional structural studies of the ErbB group of enzymes on the binding of (i) ATP or an ATP analog along with (ii) Mg^{2+} and (iii) a peptide substrate or inhibitor would provide a better understanding of their interaction with the glycine-rich loop, and such information might lead to the design of better therapeutic inhibitors.

The exocyclic amino group of ATP characteristically interacts with the peptide backbone of one or more hinge residues. Hinge residues after the β5-strand connect the small and large lobes. The 6-amino group of the adenine ring of an ATP analog (AMP-PNP, or 5′-adenylyl-β, γ-imidodiphosphate) forms hydrogen bonds with the carbonyl oxygens of EGFR Thr790 and Gln791 (PDB ID: 2ITN); Thr790 is the gatekeeper residue that occurs before the hinge region and Gln791 is the first residue of the hinge. The N-1 of the adenine ring forms a hydrogen bond with the main chain —NH group of the Met793 hinge residue and the N-3 of the adenine ring forms a hydrogen bond with a water molecule that interacts with the 1′-ribose hydroxyl group. The α-phosphate binds to Lys745 of the β3-strand, which in turn forms a salt bridge with Glu762 of the αC-helix. The γ-phosphate of ATP binds to Mg^{2+}, which coordinates with Asp854 of the DFG segment (Fig. 8). Note that the adenine base extends only to the β2 strand, but not to the β3-strand, which is in contrast to most small molecule ATP-competitive inhibitors.

4.2. Catalytic loop and activation segment

Many ATP-competitive protein kinase inhibitors interact with the peptide backbone group of hinge residues. For example, the quinazoline ring of erlotinib is oriented with its N-1 in the ATP-binding pocket of EGFR where it accepts a hydrogen bond from the main chain —NH group of the Met793 hinge residue [3]. Gefitinib and afatinib also form hydrogen bonds with Met793. These three drugs make hydrophobic contacts with Ala743, Val716, and Leu718 in the amino-terminal lobe and with Leu844 in the carboxyterminal lobe. These residues also interact with ATP, but they are omitted from Fig. 8 for the sake of clarity.

Hanks et al. identified 12 subdomains (I–VIa, VIb–XI) with conserved amino-acid-residue signatures that constitute the catalytic core of protein kinases [42]. Of these, the following four amino acids define a K/E/D/D (Lys/Glu/Asp/Asp) signature and illustrate the catalytic properties of EGFR. As noted earlier, the K (Asp) of this series occurs in the β-3 strand and forms a salt bridge with E (Glu) of the αC-helix (the E of K/E/D/D).

The catalytic loops surrounding the actual site of phosphoryl transfer consist of H/YRD$(X)_4$N. The catalytic loop HRD is the first D of K/E/D/D (Table 2). This loop consists of an H/YRDLKPEN canonical sequence in many protein serine/threonine kinases and an

Table 2
Important residues in the protein kinase domain of human ErbB receptors.[a]

	ErbB1	ErbB2	ErbB3	ErbB4
N-lobe				
Glycine-rich loop: GSGAFG	719–724	727–732	716–721	725–730
β-3 lysine (K of K/E/D/D)	745	753	742	751
αC-Glu or His (E of K/E/D/D)	E762	E770	H759	E768
αC-helix β5-strand HΦ bond	L760-I780	L768-I788	None	M766-V786
αC-β4 loop and αE helix HΦ bond	V774-Y827	V782-Y835	I771-Y824	L780-Y833
Hinge residues	791–796; QLMPFG	799–804; QLMPYG	788–793; QYLPLG	797–802; QLMPHG
C-lobe				
αE-activation segment loop and activation segment HΦ-bond[b]	R832-L862	R840-L870	None	R838-L868
Catalytic loop HRD (first D of K/E/D/D)	837	845	N834	843
Intra-catalytic loop salt bridge[b]	D837-R841	D845-R849	None	D843-R847
Catalytic loop activation segment H-bond[b]	R836-L858	R844-L866	None	R842-L864
Catalytic loop H-bond[b]	V834-R836	V842-R844	None	V840-R842
Catalytic loop asparagine (N)	842	850	839	848
Activation segment	855–884	863–892	852–881	861–890
Activation segment DFG (second D of K/E/D/D)	855	863	852	861
Mg^{2+}-positioning loop	^{855}DFGLAK^{590}	^{863}DFGLAR^{868}	^{852}DFGVAD^{857}	^{861}DFGLAR^{866}
Activation segment tyrosine phosphorylation site	869	877	868	875
Substrate protein-positioning loop	877–884	885–892	874–881	873–890
End of the activation segment: ALE	882–884	890–892	879–881	888–890
ALE E and αH-αI loop salt bridge	E884-R958	E892-R966	E881-R955	E890-R964
UniProt KB ID	P00533	P04626	P21860	Q15303

[a] Nascent residues including the signal peptide.
[b] Occurs in the active, but not dormant, kinase domain.

HRDLAARN sequence in receptor protein-tyrosine kinases including ErbB1/2/4 (Fig. 5). The catalytically impaired ErbB3 contains HRNLAARN with an asparagine (N) in place of aspartate (D). The catalytic aspartate (D845) of ErbB1 serves as a base that accepts a proton from the tyrosyl —OH group (Fig. 9). Zhou and Adams suggested that this aspartate positions the substrate hydroxyl for an in-line nucleophilic attack [44]. The asparagine within the catalytic loop (Asn842 in ErbB1) participates in the coordination of Mg^{2+} along with the DFG-aspartate.

The activation segment DFG is the second D of K/E/D/D. As noted above, this residue occurs in an active DGF-Asp in and an inactive DGF-Asp out conformation in various protein kinases. The first five residues of the activation segment constitute the Mg^{2+}-positioning loop. The activation loop contains tyrosine residues that may undergo phosphorylation, but such phosphorylation is not required for ErbB receptor activation [23,32]. The last eight residues of the ErbB/HER activation segments (PIKWMALE) make up the protein-substrate positioning segment (Fig. 9).

The activation loop and the αGHI helical subdomain are anchored firmly to the hydrophobic αF-helix by a highly conserved and buried ion pair [45]. This ion pair consists of arginine (Arg958 of nascent EGFR) that lies in the αHI loop and glutamate (Glu884), which occurs within the ALE sequence at the end of the activation loop. This ion pair serves as a hub between these two structurally conserved elements and is a defining feature of protein kinase domains. The αG and αF helical domains are stabilized by a hydrophobic bond between Tyr915 in the loop proximal to αG and Trp898 in the αF helix, which also forms a hydrophobic bond with Ile926 in the αG segment (Fig. 7).

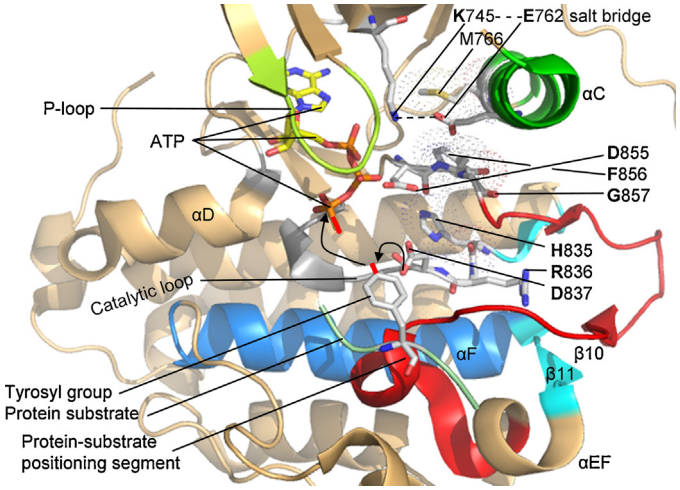

Fig. 9. Diagram of the inferred interactions between the human EGFR catalytic domain residues, ATP, and a protein substrate. D837 of the HRD catalytic loop is the base that removes the proton from the tyrosyl substrate. The phenolic oxygen of the tyrosyl residue attacks the γ-phosphate of ATP. Hydrophobic interactions between M766 of the αC-helix, F856 of the DFG motif, and H835 of the HRD motif within the catalytic loop are shown by the dots. The diagram is adapted from PDB ID: 2GS6, which depicts an ATP–peptide-substrate conjugate bound to active EGFR. The peptide, Glu–Ile–Tyr–Gly–Glu, was initially characterized as part of a synthetic Src substrate [43]. Residue numbers correspond to the nascent protein including the 24-residue signal peptide.

5. Catalytic mechanism of protein kinases

5.1. Phosphoryl transfer transition states

The catalytic mechanisms of protein kinases have been addressed by steady-state and transient kinetics, site specific mutations, quantum mechanical and molecular mechanics simulations, X-ray crystallography, and NMR spectroscopy. Most studies have been performed with PKA, and there is a general consensus that these fundamentals will hold for other protein kinases. However, each class of protein kinase is expected to exhibit its unique variations from the reaction template. The transfer of the phosphoryl group of ATP to a substrate is a substitution reaction centered on phosphorus [46]. Ho et al. demonstrated that such transfers as catalyzed by PKA proceed with inversion of configuration at the terminal phosphorus atom [47]; this finding indicates that the enzymatic mechanism involves a nucleophilic substitution. This is perhaps the most direct experiment shedding light on the catalytic mechanism of protein kinases because of ambiguity and discordant findings in other mechanistic studies.

A reaction mechanism is symbolized by dividing it into elementary steps. A_N is used to represent nucleophilic addition and D_N

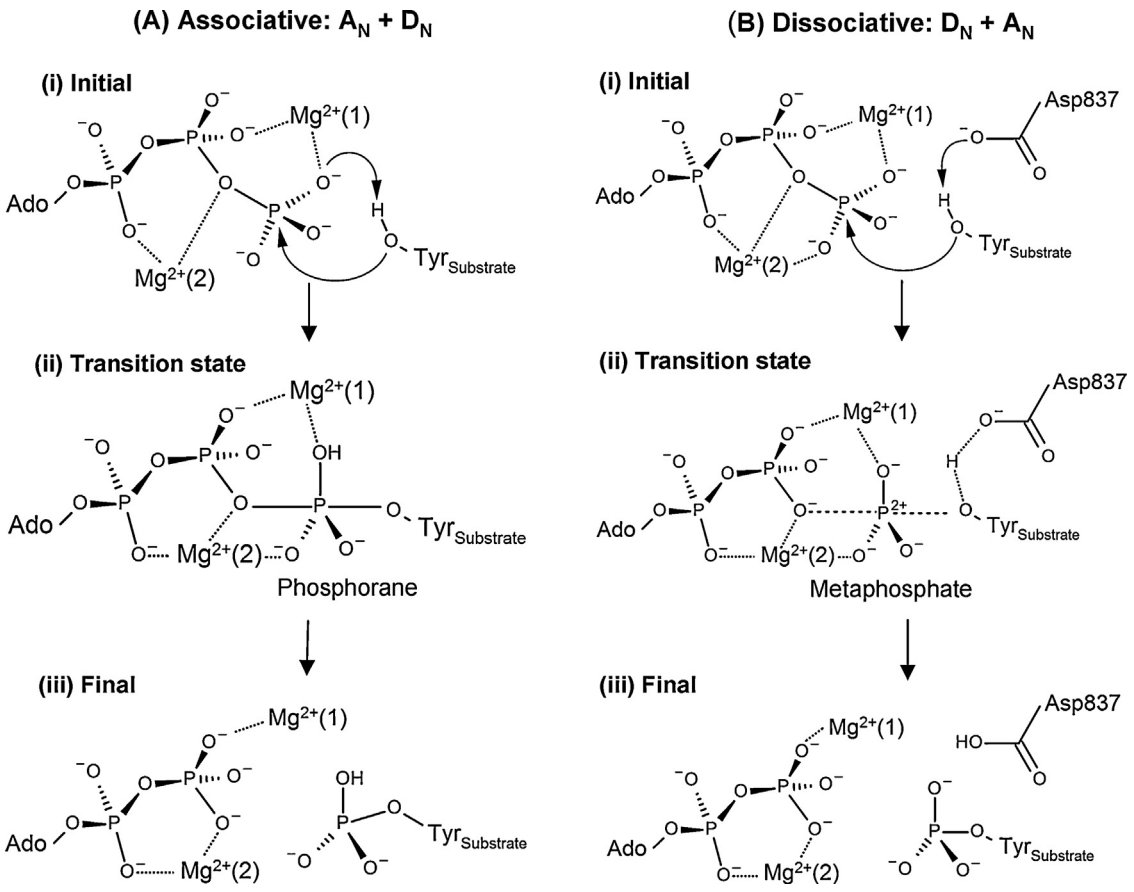

Fig. 10. EGFR protein kinase associative and dissociative reaction mechanisms. A_N represents nucleophilic addition and D_N represents nucleofuge dissociation. The two different magnesium ion binding sites are represented by $Mg^{2+}(1)$ and $Mg^{2+}(2)$. Ado, adenosine.

is used to represent nucleofuge dissociation, where nucleofuge is a leaving group that retains the bonding electron pair [48]. When D_N and A_N occur in separate steps and a discrete intermediate is formed, the terms are separated. For example, if the intermediate is long-lived enough to diffusionally separate from the leaving group, the terms are separated by a plus sign ($D_N + A_N$). Hengge reviewed two reaction mechanisms proposed for the phosphoryl transfer catalyzed by protein kinases; these are (i) associative or (ii) dissociative [46]. The main differences between these mechanisms are the transitions states and the group that accepts the proton from the protein substrate residue.

All chemical reactions pass through an unstable structure called the transition state, which is poised between the chemical structures of the reactants and products [49,50]. The transition state represents a complex where chemical bonds are being made and broken. It is an energized state with a fleeting existence ($\approx 10^{-12}$–10^{-13} s), the time required for a single bond vibration. The transition state in the associative process is trigonal bipyramidal where bond formation with the substrate begins before the bond between the β- and γ-phosphate is completely broken. The transition state contains a phosphorane moiety with a valence of five (Fig. 10). The proton on the substrate residue is accepted by the incoming phosphate. The dissociative mechanism involves a complete break in the leaving group yielding a metaphosphate with a −1 charge. The conserved catalytic HRD aspartate (Asp837 in EGFR) is proposed to act as a catalytic base that accepts the proton from the substrate residue. In the dissociative transition state, bond breaking between the phosphorus center and the leaving group (ADP) is more advanced than bond making with the incoming phenolic oxygen of tyrosine. Although there is evidence for each of these mechanisms, the preponderance of recent data suggests that the protein kinase catalyzed reaction involves the dissociative process [51,52].

Bao et al. determined the structure of the transition state of CDK using ADP, Mg^{2+}, a peptide substrate, and MgF_3^- [53]. MgF_3^- mimics the γ-phosphate in the transition state of ATP-requiring reactions. Pauling proposed that the large rate acceleration of enzymes is caused by the high specificity of the protein catalyst for binding, not the substrate, but rather the substrate molecule in a strained configuration corresponding to the activated complex with only a transient existence (the transition state in contemporary terminology) [54,55]. Pauling hypothesized that the enzyme would attract the substrate molecules and deform them into the configuration of the activated complex, for which the power of attraction by the enzyme is greatest. He thought that this idea could be tested by searching for inhibitors that have a greater power of combination with the enzyme than with the substrate molecules themselves. Thus, transition state analogs are inhibitors designed to exploit the special interactions that distinguish the substrate in the transition state from the substrate in the ground state. The observation that stable analogs of the transition states for enzymatic reactions often act as tight-binding inhibitors provide support for this proposal [49]. It would be helpful to have structural studies of the transition states of the ErbB family that could be used for the development of inhibitory transition state analogs.

5.2. Transition state analogs and drug development

Synthesis of transition-state analogs has led to the development of two classes of FDA-approved drugs: one class targets human

Table 3
Effect of high Mg^{2+} concentrations on steady-state kinetic parameters of various protein kinases.

Enzyme	Class	Specificity	Substrate	V_{max}	K_{MgATP}	V_{max}/K_{MgATP}	References
Bovine PKA	Non-receptor	Ser/Thr	LRRASLG	↓	↓	↑	[60]
Human CDK2	Non-receptor	Ser/Thr	Histone H1	↓	↓	↑	[61]
Human CDK5	Non-receptor	Ser/Thr	PKTPKKAKKL	↑	↓	↑	[62]
Rat ERK2	Non-receptor	Ser/Thr	Ets138	↑	↓	↑	[63]
Human Csk	Non-receptor	Tyr	Poly-E_4Y	↑	No Δ	↑	[64]
Chicken Src	Non-receptor	Tyr	Poly-E_4Y	↑	No Δ	↑	[64]
Xenopus fibroblast growth factor receptor-1	Receptor	Tyr	Poly-E_4Y	↑	↓	↑	[64]
Rat insulin receptor	Receptor	Tyr	Poly-E_4Y	No Δ	↓	↑	[65]
Avian v-Fps	Receptor	Tyr	EAEIYEAIE	No Δ	↓	↑	[66]

immunodeficiency virus and the second targets the influenza virus [56]. The maturation of the AIDS human immunodeficiency virus requires the proteolytic conversion of glycosaminoglycan (gag) and gag-polymerase into structural and functional proteins. Inhibition of this process blocks viral replication. HIV protease inhibitors have been tailored to the peptidic linkages in the HIV precursor proteins that are cleaved by the protease. Using the X-ray crystallographic structure, inhibitors have been modeled in the active site of the protease, which is formed at the interface of two homodimeric subunits and contains two catalytic aspartate residues. Saquinavir, which is a transition-state analog of an HIV proteinase-cleavage site, is a potent and orally effective FDA-approved inhibitor of HIV-1 and HIV-2 proteinases that is used for the treatment of AIDS [57].

The substrates for HIV protease are specific peptide bonds: R—C(=O)—N(H)—R′. The transition state used is modeled after hydroxyethylamine: R—CH(OH)—CH_2—N(H)—R′. The hydroxyethylamine derivatives are not cleaved by the protease. The methylene —CH_2— spacer converts the substrate-like compound into a transition-state analog intermediate between the peptide substrate and the two peptide products. Several FDA-approved protease inhibitors used in the treatment of AIDS are transition-state analogs, including first generation (saquinavir, indinavir, nelfinavir, lopinavir, ritonavir, fosamprenavir, and tipranavir) and second generation inhibitors (atazanavir and darunavir) [58]. Furthermore, oseltamivir and zanamivir are orally effective drugs that are used in the treatment of influenza infection. Both compounds are transition-state analogs that were tailored to interact with conserved amino-acid residues within the active site of viral neuraminidase as determined by X-ray crystallography and computational chemistry [58].

5.3. Role of the magnesium ion in the protein kinase catalytic process

The role of divalent cations such as Mg^{2+} in protein kinase-mediated reactions is intricate. Using nuclear magnetic resonance and steady-state kinetic studies, Armstrong et al. reported that the catalytic subunit of PKA in the presence of a nucleotide such as ADP contains two binding sites for Mn^{2+} (K_d = 6–10 μM and 50–60 μM) or for Mg^{2+} (both about 1.6 mM) [59]. In the absence of a nucleotide, divalent cation binding affinity is nil. They demonstrated that increasing the Mn^{2+} concentration first increases the reaction rate, but further increases (Mn^{2+} > 75 μM) lead to a progressive decline in the reaction rate. They reported that the more tightly bound Mn^{2+} is an essential metal ion activator while the more weakly bound Mn^{2+} is an inhibitor of catalytic activity. Our steady-state kinetic analysis of PKA indicated that MgATP and peptide substrate bound to the enzyme in random order with the ordered release of phosphopeptide and then MgADP [60]. We found that increasing the concentration of Mg^{2+} results in a V_{max} that is about one-fifth that at low (0.5 mM) Mg^{2+} concentrations. Even though these studies led to the terminology of an inhibitory Mg^{2+} site, the catalytic efficiency (V_{max}/K_{MgATP}) at high Mg^{2+} concentration increases by 13-fold as a result of the decreased K_{MgATP}.

The role of divalent cations including Mg^{2+} has been examined in other protein kinases including CDK and ERK2 (protein-serine/threonine kinases), Csk and Src (non-receptor protein-tyrosine kinases), and fibroblast growth factor receptor, insulin receptor, and v-Fps protein tyrosine kinases. Variable effects on the V_{max} and K_{MgATP} have been observed. In all cases, however, the kinetic efficiency (V_{max}/K_{MgATP}) increases (Table 3). The V_{max}/K_{MgATP} is an apparent second-order rate constant ($M^{-1}\,s^{-1}$) that relates the reaction rate to the concentration of free, rather than total, enzyme (this discussion ignores the protein substrate of protein kinases). At low substrate concentrations the enzyme is largely unbound, or free, and the reaction velocity is given by $v = [E][MgATP] \times V_{max}/K_{MgATP}$ [67]. This constant (V_{max}/K_{MgATP}) is called the specificity constant when it is used to compare the effectiveness of multiple substrates for a given enzyme. For enzyme reactions that are limited only by diffusion of the substrate and enzyme, the upper limit of the value of the kinetic efficiency is $\approx 10^8\,M^{-1}\,s^{-1}$. Its value for the catalytic subunit of bovine PKA is $2.3 \times 10^5\,M^{-1}\,s^{-1}$ [60] and that for human Csk is $500\,M^{-1}\,s^{-1}$ [64]. Unlike general metabolic enzymes, protein kinases function as dynamic molecular switches that are turned on or off. Protein kinases are not continuously active as, for example, hexokinase [33]. Thus a very low catalytic efficiency for protein kinases is not detrimental and is consistent with their physiological functions. Although one of the Mg^{2+} binding sites is labeled inhibitory, this is somewhat of a misnomer because the kinetic efficiency is uniformly increased.

In contrast to the above studies, Mukherjee et al. reported that Ca^{2+}/calmodulin-activated Ser–Thr kinase (CASK) functions without a divalent cation [68]. This enzyme, which lacks the critical D of DFG, was thought to be an inactive pseudokinase. However, this enzyme exhibits catalytic activity and, surprisingly, catalysis is actually inhibited by Mg^{2+}, Mn^{2+}, or Ca^{2+}. In another study, Gerlits et al. reported that PKA can mediate the phosphorylation of a high affinity peptide (SP20) in the absence of a divalent cation [69]. The latter study demonstrated that divalent metals greatly enhance catalytic turnover. Moreover, in the absence of Mg^{2+} or other metal, these investigators showed that PKA mediates but a single turnover from ATP to a tight-binding substrate (SP20).

Zheng et al. determined the X-ray crystal structure of the catalytic subunit of murine PKA bound to Mg^{2+}, ATP, and a heat stabile protein kinase inhibitor that mimics a protein substrate [70]. Crystals were prepared under low [Mg^{2+}] and high [Mg^{2+}] conditions. They reported that MgATP is sandwiched between the small and large lobes. Under low [Mg^{2+}] conditions, a single Mg^{2+} is bound to the β and γ-phosphates and to the aspartate of the DFG sequence; this magnesium ion is labeled 1: Mg^{2+} (1). Under high [Mg^{2+}] conditions, a second Mg^{2+} is bound to the α and γ-phosphates and to the asparagine amide nitrogen within the catalytic loop downstream from the Y/HRD conserved sequence. This magnesium ion is labeled 2: Mg^{2+}(2).

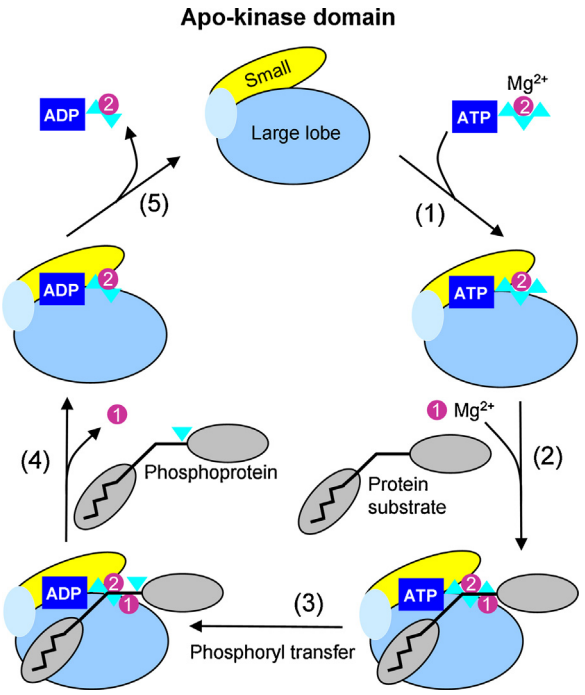

Fig. 11. Proposed protein kinase catalytic cycle including $Mg^{2+}(1)$, $Mg^{2+}(2)$-ATP, and $Mg^{2+}(2)$-ADP.
Source: Adapted from Bastidas et al. [73].

The potential role of each of the Mg^{2+} ions has been the subject of numerous investigations during the past two decades. For many years investigators thought that $Mg^{2+}(1)$ was the essential divalent cation that participates in protein kinase reactions [71]. Jacobsen et al. used steady-state kinetics, X-ray crystallography, and molecular dynamics simulations to investigate the role of two cations in the CDK-mediated reaction [61]. They demonstrated that the simultaneous binding of two Mg^{2+} ions is essential for efficient phosphoryl transfer. Their studies indicate that ADP phosphate mobility is more restricted when ADP is bound to two Mg^{2+} ions when compared to one. The cost that is paid to accelerate the chemical process is the limitation in the rate of ADP release, which is the rate-limiting step in the overall process [44,72]. Jacobsen et al. hypothesize that $Mg^{2+}(1)$ is released prior to ADP-$Mg^{2+}(2)$ [61].

Bastidas et al. performed X-ray crystallographic studies with the catalytic subunit of murine PKA, Mg^{2+}, and an ATP analog (AMP-PNP) [73]. This is a stable analog that ordinarily fails to react; however, these investigators found that the analog transfers its terminal phosphoryl group to a peptide substrate. They examined a crystal structure that contained 55% intact AMP-PNP and an unphosphorylated peptide substrate and 45% displaying transfer of the γ-phosphoryl group onto the substrate peptide yielding AMP-PN and a phosphorylated peptide. These structures implicate $Mg^{2+}(2)$ as the more stably bound ion. Following the transfer reaction, $Mg^{2+}(2)$ recruits a water molecule to retain its octahedral coordination geometry and it remains in the active site while $Mg^{2+}(1)$ is released. Until the work of Jacobsen et al. [61] and Bastidas et al. [73], the evidence seemed to indicate that $Mg^{2+}(2)$ was released first and $Mg^{2+}(1)$ was released afterward [71,72].

The catalytic cycle for protein kinases suggested by both Jacobsen et al. [61] and Bastidas et al. [73] is summarized in Fig. 11. $Mg^{2+}(2)$-ATP binds to the free kinase domain. $Mg^{2+}(1)$ and the protein substrate bind, but the order of their binding is unclear. The enzyme then catalyzes the transfer of the phosphoryl group to the protein substrate. $Mg^{2+}(1)$ and the phosphorylated protein substrate are released, but the order of their release is unclear. $Mg^{2+}(2)$-ADP is released during the last and rate-limiting step of the process. Bastidas et al. suggest that the mechanism of all protein kinases will require two magnesium ions for catalysis [73]. So far there are no steady-state or transient-state kinetic studies with the ErbB family to corroborate this hypothesis. Furthermore, additional X-ray crystallographic work with bound nucleotide and high $[Mg^{2+}]$ are needed to establish a role for two magnesium ions in ErbB biochemistry.

The elucidation of the role of the two Mg^{2+} ions, if applicable for the ErbB family, suggests another strategy for the development of inhibitory drugs. In the case of ErbB1, $Mg^{2+}(2)$-ATP would be bound by the invariant Asn842 within the catalytic loop. The design of ligands that bind to the ATP-binding pocket with an extension that interacts with this asparagine promises to yield a new type of kinase inhibitor. Peng et al. have developed some EGFR inhibitors that form a salt bridge with Asp831 of the DFG-motif [74]. This class of drugs may interfere with the binding of $Mg^{2+}(1)$ to the enzyme.

6. Therapeutic small molecule inhibitors of the ErbB/HER protein kinases

6.1. Mutant ERBB1 oncogenic activation

ErbB1/EGFR plays an important role in the pathogenesis of many lung cancers. Herbst et al. reported that *EGFR* kinase-domain mutations occur in a range of 10–40% of lung cancer samples [75]. The incidence of *EGFR* kinase-domain mutations is about 10% in Caucasian populations and 30–40% in Asian patients. About 10% of unselected patients with NSCLC exhibited rapid and often dramatic responses to gefitinib [76]. In 2004, three groups compared the tumors of patients who responded to gefitinib with nonresponders [76–78]. Each of the groups reported that most of the responders possessed mutations of the *EGFR* kinase domain while those of nonresponders lacked *EGFR* gene mutations. The most common mutations that these groups discovered were (i) the deletion of five exon-19 residues (^{746}Glu–Leu–Arg–Glu–Ala^{750}) that occur immediately before the αC-helix and (ii) the exon-21 substitution of an arginine for leucine (Leu858Arg) in the activation segment (residue numbers include the signal peptide). Together, these two mutations account for more than 90% of the activating *EGFR* mutations observed in NSCLC. Pao et al. reported patients who responded to erlotinib also possessed these *EGFR* mutations [80]. The ^{719}Gly–Cys–Ala–Arg–Asp–Val–Ser^{725} P-loop mutations account for about 3% of the activating *EGFR* gene mutations. Altogether, more than 200 *EGFR* mutations have been described in NSCLC (www.somaticmutations-egfr.org) [79]. The FDA approved gefitinib for the treatment of NSCLC in 2003 [80] and erlotinib in 2004 [81].

The activating mutations of oncokinases generally occur in or near important regulatory regions such as the αC-helix, the activation segment, or the phosphate binding loop. A general mechanism for the oncogenic activation of the ErbB family of receptors involves the destabilization of the dormant resting state, which promotes the formation of the active state. Yun et al. documented this destabilization as the mechanism responsible for the activation of EGFR for the Leu858Arg and Gly791Ser mutants (residue numbers including the signal peptide) [82]. The Leu858Arg mutation lies in the amino-terminal portion of the activation segment; it immediately follows the ^{855}DFG^{857} sequence that marks the beginning of the activation segment. The substitution of the larger positively charged arginine side chain for the hydrophobic leucine side chain prohibits its occurrence in the dormant closed activation segment while it is readily accommodated in the active open conformation of the EGFR protein kinase domain [82]. They hypothesized that the

Leu860Gln activation segment mutant that occurs in gefitinib and erlotinib-responsive NSCLCs is activated by a similar mechanism.

Red Brewer et al. characterized the interaction of the Leu834Arg activated mutant and the Leu834Arg/Thr766Met drug-resistant double mutant with wild type EGFR or ErbB2 [83]. Based upon co-immunoprecipitation assays, they reported that the Leu834Arg mutant and drug-resistant double mutant enhance the strength of the donor/acceptor receptor interaction. They determined the X-ray crystal structure of the Leu834Arg/Thr766Met double mutant and observed that the enzyme forms an asymmetric dimer similar to that observed with EGFR. Their experiments support the notion that these activated *EGFR* mutants preferentially serve as acceptors in the asymmetric dimer resulting in *EGFR* mutant activation. The authors noted that the Leu834Arg mutation or the Leu834Arg/Thr766Met double mutation destabilizes the inactive conformation, and the energetic cost of inducing the active conformation of the acceptor kinase is lower in the mutants than in the wild type enzymes.

6.2. FDA-approved small molecule ErbB kinase domain inhibitors

Erlotinib and afatinib are FDA-approved EGFR inhibitors that are used in the treatment of NSCLC bearing *EGFR* mutations [80,81]. Gefitinib was used in the treatment of NSCLC *EGFR* mutants in the United States. Although its FDA approval has been withdrawn, the drug is still approved for this treatment in dozens of countries worldwide. Moreover, lapatinib is a combination ErbB1 and ErbB2 FDA-approved inhibitor that is used in the treatment of ErbB2-overexpressing breast cancers [84]. Lapatinib is currently in clinical trials for the treatment of colorectal and gastroesophageal cancers and other solid tumors (www.clinicaltrials.gov).

Nearly all NSCLC patients with EGFR-activating mutations develop resistance to gefitinib or erlotinib after a median duration of 10–13 months [85]. The most common mechanism for resistance, which occurs in 50–60% of patients, is the development of a Thr790Met gatekeeper mutation in exon 20 [86]. This mutation replaces threonine with the larger methionine near the ATP-binding site. Afatinib is a quinazoline derivative that readily fits into the ATP-binding pocket and irreversibly inhibits the activated (Leu858Arg) Thr790Met gatekeeper mutant suggesting that the substitution of the larger for smaller residue does not sterically block drug binding [87]. Moreover, Yun et al. directly demonstrated that the activating Leu858Arg mutant, the Thr790Met mutant, and the double mutant bind gefitinib more tightly than the wild type enzyme [88]. They found that the K_m for ATP is increased in the Leu858Arg mutant when compared with the wild type enzyme, but the second Thr790Met mutation decreases the K_m for ATP, which increases its ability to compete with gefitinib for binding and decreases the inhibitory effect of the drug *in vivo*. A methionine in the gatekeeper position may also stabilize the hydrophobic spine [89], which may lead to greater activity of the EGFR Leu858Arg/Thr790Met double mutant. Engelman et al. reported an additional mechanism of resistance to gefitinib or erlotinib, which occurs in about 22% of patients, that is related to the up regulation of the hepatocyte growth factor receptor, or c-Met [90]. These investigators reported that *MET* amplification produces ErbB3-dependent activation of the phosphoinositide 3-kinase pathway.

Afatinib is approved by the FDA for the first-line treatment of NSCLC in patients bearing the activating (i) exon-19 deletions or (ii) the Leu858Arg mutation. This drug also inhibits the Leu858Arg/Thr790Met double mutant [91] and thus may represent an effective therapy for patients who have developed resistance to erlotinib or gefitinib. Crizotinib is an FDA-approved drug for the treatment of ALK-positive NSCLC [92]. Crizotinib was initially developed as an inhibitor of c-Met, and it may prove efficacious in the treatment of patients with *MET* amplification resulting from erlotinib or gefitinib treatment.

6.3. ErbB family inhibitors under development and in clinical trials

The efficacy of several drugs that target the ErbB family pathways are undergoing evaluation in numerous clinical trials (Table 4), and many more ErbB family inhibitors are under development throughout the world. Afatinib is an irreversible ErbB1 inhibitor that is approved for the treatment of NSCLC and is currently undergoing clinical trials for the treatment of breast, colorectal, esophageal, and head and neck cancers (www.clinicaltrials.gov). Vandetanib is a multiprotein kinase inhibitor (ErbB1/VEGFR1/RET), which is approved for the treatment of medullary thyroid cancer, and is in clinical trials for the treatment of NSCLC and head and neck squamous cell carcinoma. Neratinib is ineffective in the treatment of NSCLC, but it is still being studied as an agent for the treatment of breast cancer. Although it is an irreversible inhibitor of ErbB1 like afatinib, neratinib seems to be ineffective in the treatment of the Thr790Met mutants of activated ErbB1. Of the agents listed in Table 4, more studies have been

Table 4
Selected small molecule inhibitors of the ErbB family of protein kinases.

Name	Target	PubChem CID[a]	Cancer indications	Scaffold	References
FDA-approved ErbB kinase inhibitors					
Afatinib[b]	ErbB1	10184653	NSCLC	Quinazoline	[87,93]
Erlotinib	ErbB1	176870	NSCLC	Quinazoline	[78,81,94]
Gefitinib	ErbB1	123631	NSCLC	Quinazoline	[78,80,94]
Lapatinib	ErbB1/2	208908	Breast	Quinazoline	[95,96]
ErbB kinase inhibitors in clinical trials					
AZD-9291	ErbB1	Not assigned	NSCLC	Indolepyrimidine	Clinicaltrials.gov
BMS-599626	ErbB1/2/4	10437018	Glioma	Pyrrolotriazine	[97]
Canertinib[b]	ErbB1/2	156413	NSCLC/breast	Quinazoline	[98]
Dacomitinib[b]	ErbB1/2/4	11511120	NSCLC/gastric/head and neck/glioma	Quinazoline	[99–102]
Icotinib	ErbB1	44609731	NSCLC	Quinazoline	[103–106]
Neratinib[b]	ErbB1/2	9915743	Breast/NSCLC	Anilinoquinoline	[107,108]
Poziotinib[b]	ErbB1/2/4	25127713	NSCLC/breast/gastric	Anilinoquinoline	[109–111]
TAK-285	ErbB1/2	11620908	Advanced solid tumors	Pyrrolopyrimidine	[112,113]
Vandetanib[c]	ErbB1/VEGFR/RET	3081361	Thyroid/NSCLC/head and neck	Quinazoline	[104,114]
WZ4002[b]	ErbB1	44607530	NSCLC	Anilinopyrimidine	[115]

[a] The PubChem CID (chemical identification no.) from the National Library of Medicine (http://www.ncbi.nlm.nih.gov/pubmed) provides the chemical structure, molecular weight, number of hydrogen-bond donors/acceptors, and bibliographic references.
[b] Irreversible.
[c] FDA-approved RET inhibitor used for the treatment of medullary thyroid carcinoma.

performed with dacomitinib than the other drugs. In preclinical studies, it was effective in blocking *EGFR*-drug resistant mutants [90]. Its effects against the drug resistant Thr790Met mutant in patients, however, were observed in some cases but not in others. Although early studies with canertinib appeared promising, it has been discontinued from clinical development.

6.4. Comparison of erlotinib and lapatinib binding to EGFR

Erlotinib is an inhibitor of EGFR and is approved by the FDA for the treatment of NSCLC in patients bearing activating *ERBB1* mutations. Lapatinib is an inhibitor of ErbB1/2 and is approved for the treatment of breast cancer in patients overexpressing ErbB2 [95,96]. Both of these quinazoline derivatives are reversible ATP-competitive inhibitors of EGFR (Fig. 12). The quinazoline heterocyclic group binds in the ATP-binding pocket and forms a hydrogen bond with the —NH group of Met793 in the hinge region. Erlotinib binds to the active conformation while lapatinib binds to the displaced inactive αC-out conformation of EGFR. A comparison of the superposed structures of erlotinib, lapatinib, and an ATP-analog (AMP-PNP) that bind to EGFR are depicted in Fig. 12C and D.

The anilino group of erlotinib or lapatinib extends into a hydrophobic region of the kinase domain of EGFR that is adjacent to the adenine-binding site (the back pocket). This hydrophobic site extends only to the β5-sheet containing the Thr790 gatekeeper residue and to Thr855 on top of the activation segment (Fig. 12E). The anilino group of lapatinib contains a 3-fluorophenylmethoxy (3-FPM) group extension that displaces the αC-helix to its out position. As a result of the larger size of lapatinib, the hydrophobic pocket next to the adenine-binding site extends to the β4-sheet (Leu778), the αC-helix (Met766), the top of the β7-activation segment loop (Leu856), and the activation segment (Phe856).

Sánchez-Martín and Pandiella compared ligand-induced ErbB2-ErbB3 heterodimer formation in cell lines following treatment by canertinib, erlotinib, gefitinib, lapatinib, neratinib, and pelitinib using co-immunoprecipitation and Förster resonance energy transfer assays [116]. Lapatinib and neratinib are dual ErbB1/2 inhibitors while canertinib and pelitinib are ErbB1/2/4 inhibitors. In contrast, erlotinib and gefitinib are classical ErbB1 inhibitors. However, these investigators used high concentrations (5 μM) of all of these drugs and each blocked ErbB2 phosphorylation, which suggests that erlotinib and gefitinib inhibited multiple ErbB family protein kinases under their experimental conditions.

Sánchez-Martín and Pandiella found that lapatinib and neratinib inhibited heterodimer formation in response to Nrgβ-1 in human MCF7 breast cancer cells whereas the other agents did not [116]. They also found that lapatinib and neratinib, but not pelitinib, disrupted heterodimers that had formed in response to Nrgβ-1. Lapatinib and neratinib (an irreversible ErbB1 inhibitor with a large side chain attached to a quinoline scaffold), but not gefitinib or neratinib, prevented receptor heterodimerization and augmented antibody-mediated cytotoxicity.

They attributed these differential effects to the different modes of inhibitor binding to the ErbB family: they suggested that canertinib, erlotinib, gefitinib, and pelitinib (which have a small derivative attached to the scaffold) bind to the active kinase domain (αC-in) while lapatinib and neratinib bind to the inactive conformation (αC-out). These investigators suggested that binding to the αC-out enzyme configuration prevents these complexes from acting as the acceptor kinase in the asymmetric dimer and are thus unable to be activated as described in Section 2.2. The larger drugs (lapatinib and neratinib) thus inhibit ErbB activity by (i) preventing activation and (ii) by blocking ATP binding while the smaller

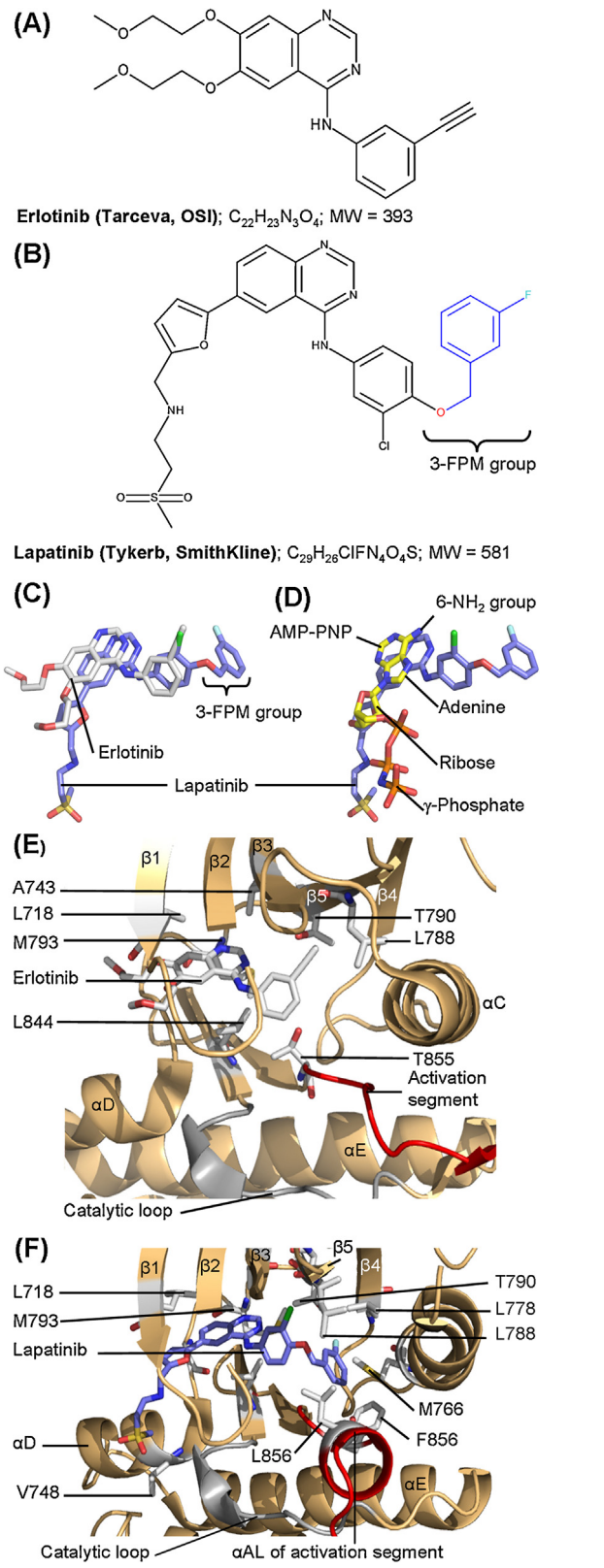

Fig. 12. Comparison of erlotinib and lapatinib binding to EGFR. (A) Erlotinib. (B) Lapatinib. (C) Superposition of erlotinib (gray carbon atoms) and lapatinib (blue carbon atoms) bound to EGFR as determined from PDB ID: 1M17 and 1XKK, respectively. (D) Superposition of AMP-PNP (yellow carbon atoms) and lapatinib (blue carbon atoms) bound to EGFR as determined from PDB ID: 3VJO and 1XKK, respectively. (E) Binding of erlotinib to the active form (αC-in) of EGFR (PDB ID: 1M17). (F) Binding of lapatinib to the inactive form (αC-out) of EGFR (PDB ID: 1XKK). 3-FPM, 3-fluorophenylmethoxy.

drugs have only the latter effect. Despite these differences, ErbB drug resistance to lapatinib readily occurs in the clinic [107].

7. Epilog

The ErbB family of receptor protein-tyrosine kinases participates in the pathogenesis of several common malignancies listed in Section 1.2. Several small molecule ErbB kinase domain inhibitors have been approved by the FDA for the treatment of lung cancer (afatinib, erlotinib, and lapatinib) and breast cancer (lapatinib). Furthermore several biopharmaceutical agents have been approved for the treatment of breast (pertuzumab, trastuzumab, and ado-trastuzumab emtansine) and colorectal cancer (cetuximab, panitumumab). A major shortcoming of all of these treatments is the development of resistance. Major efforts are underway to develop alternate inhibitors that are effective against the drug-resistant tumors.

Extensive studies have been performed on the nature of the biochemistry, structure, cell biology, and pharmacology of the ErbB family. However, information on several fundamental aspects of these proteins is lacking. For example, the effect of varying the Mg^{2+} ion concentration on the activity of these enzymes is needed. If two Mg^{2+} ions per kinase domain are required for activity, this suggests that the DFG-aspartate and the asparagine of the catalytic loop potentially represent bona fide inhibitory targets as noted in Section 5.3. To complement this work, X-ray structural studies of these enzymes performed under conditions of high Mg^{2+} ion concentration with ATP or an ATP analog such as AMP-PNP without and with a defined peptide substrate or peptide inhibitor. The three-dimensional structure of a transition-state analog with the ErbB enzymes might provide clues that would lead to the identification of new classes of inhibitory drugs. In the case of PKA, studies of the active enzyme with ATP indicate that residues in the glycine-rich P-loop intimately interact with the substrate nucleotide phosphates. In the case of ErbB1, X-ray studies with AMP-PNP do not reveal such interaction. However, these studies were performed at low Mg^{2+} concentrations where such interactions may be lacking. A better understanding of the fundamentals of ErbB family mechanism, structure, and function promises to aid in the discovery of new therapeutic agents for a wide variety of diseases.

Conflict of interest

The author is unaware of any affiliations, memberships, or financial holdings that might be perceived as affecting the objectivity of this review.

Acknowledgments

The author thanks Prof. John Kuriyan for providing the protein data bank file for the EGFR asymmetric dimer. He also thanks Laura M. Roskoski for providing editorial and bibliographic assistance.

References

[1] Lemmon MA, Schlessinger J. Cell signaling by receptor tyrosine kinases. Cell 2010;141:1117–34.
[2] Carpenter G, Cohen S. Epidermal growth factor. J Biol Chem 1990;265:7709–12.
[3] Roskoski Jr R. The ErbB/HER family of protein-tyrosine kinases and cancer. Pharmacol Res 2014;79:34–74.
[4] Manning G, Whyte DB, Martinez R, Hunter T, Sudarsanam S. The protein kinase complement of the human genome. Science 2002;298:1912–34.
[5] Alonso A, Sasin J, Bottini N, Friedberg I, Friedberg I, Osterman A, et al. Protein tyrosine phosphatases in the human genome. Cell 2004;117:699–711.
[6] Cohen P. Protein kinases – the major drug targets of the twenty-first century? Nat Rev Drug Discov 2002;1:309–15.
[7] Roskoski Jr R. ERK1/2 MAP kinases: structure, function, and regulation. Pharmacol Res 2012;66:105–43.
[8] Rask-Andersen M, Masuram S, Schiöth HB. The druggable genome: evaluation of drug targets in clinical trials suggests major shifts in molecular class and indication. Annu Rev Pharmacol Toxicol 2014;54:9–26.
[9] Schechter AL, Stern DF, Vaidyanathan L, Decker SJ, Drebin JA, Greene MI, et al. The neu oncogene: an erb-B-related gene encoding a 185,000-Mr tumour antigen. Nature 1984;312:513–6.
[10] Ullrich A, Coussens L, Hayflick JS, Dull TJ, Gray A, Tam AW, et al. Human epidermal growth factor receptor cDNA sequence and aberrant expression of the amplified gene in A431 epidermoid carcinoma cells. Nature 1984;309:418–25.
[11] Ghosh R, Narasanna A, Wang SE, Liu S, Chakrabarty A, Balko JM, et al. Trastuzumab has preferential activity against breast cancers driven by ERBB2 homodimers. Cancer Res 2011;71:1871–82.
[12] Shi F, Telesco SE, Liu Y, Radhakrishnan R, Lemmon MA. ErbB3/HER3 intracellular domain is competent to bind ATP and catalyze autophosphorylation. Proc Natl Acad Sci USA 2010;107:7692–7.
[13] Tzahar E, Waterman H, Chen X, Levkowitz G, Karunagaran D, Lavi S, et al. A hierarchical network of interreceptor interactions determines signal transduction by Neu differentiation factor/neuregulin and epidermal growth factor. Mol Cell Biol 1996;16:5276–87.
[14] Graus-Porta D, Beerli RR, Daly JM, Hynes NE. ErbB-2, the preferred heterodimerization partner of all ErbB receptors, is a mediator of lateral signaling. EMBO J 1997;16:1647–55.
[15] Pinkas-Kramarski R, Soussan L, Waterman H, Levkowitz G, Alroy I, Klapper L, et al. Diversification of Neu differentiation factor and epidermal growth factor signaling by combinatorial receptor interactions. EMBO J 1996;15:2452–67.
[16] Schlessinger J, Ligand-induced. receptor-mediated dimerization and activation of EGF receptor. Cell 2002;110:669–72.
[17] Ogiso H, Ishitani R, Nureki O, Fukai S, Yamanaka M, Kim JH, et al. Crystal structure of the complex of human epidermal growth factor and receptor extracellular domains. Cell 2002;110:775–87.
[18] Garrett TP, McKern NM, Lou M, Elleman TC, Adams TE, Lovrecz GO, et al. Crystal structure of a truncated epidermal growth factor receptor extracellular domain bound to transforming growth factor α. Cell 2002;110:763–73.
[19] Arkhipov A, Shan Y, Das R, Endres NF, Eastwood MP, Wemmer DE, et al. Architecture and membrane interactions of the EGF receptor. Cell 2013;152:557–69.
[20] Burgess AW, Cho HS, Eigenbrot C, Ferguson KM, Garrett TP, Leahy DJ, et al. An open-and-shut case? Recent insights into the activation of EGF/ErbB receptors. Mol Cell 2003;12:541–52.
[21] Nolen B, Taylor S, Ghosh G. Regulation of protein kinases; controlling activity through activation segment conformation. Mol Cell 2004;15:661–75.
[22] Biscardi JS, Maa MC, Tice DA, Cox ME, Leu TH, Parsons SJ. c-Src-mediated phosphorylation of the epidermal growth factor receptor on Tyr845 and Tyr1101 is associated with modulation of receptor function. J Biol Chem 1999;274:8335–43.
[23] Gotoh N, Tojo A, Hino M, Yazaki Y, Shibuya M. A highly conserved tyrosine residue at codon 845 within the kinase domain is not required for the transforming activity of human epidermal growth factor receptor. Biochem Biophys Res Commun 1992;186:768–74.
[24] Zhang X, Gureasko J, Shen K, Cole PA, Kuriyan J. An allosteric mechanism for activation of the kinase domain of epidermal growth factor receptor. Cell 2006;125:1137–49.
[25] Jin L, Wang W, Fang G. Targeting protein–protein interaction by small molecules. Annu Rev Pharmacol Toxicol 2014;54:435–56.
[26] Roskoski Jr R. RAF protein-serine/threonine kinases: structure and regulation. Biochem Biophys Res Commun 2010;399:313–7.
[27] Hatzivassiliou G, Song K, Yen I, Brandhuber BJ, Anderson DJ, Alvarado R, et al. RAF inhibitors prime wild-type RAF to activate the MAPK pathway and enhance growth. Nature 2010;464:431–5.
[28] Knighton DR, Zheng JH, Ten Eyck LF, Ashford VA, Xuong NH, Taylor SS, et al. Crystal structure of the catalytic subunit of cyclic adenosine monophosphate-dependent protein kinase. Science 1991;253:407–14.
[29] Seeliger MA, Ranjitkar P, Kasap C, Shan Y, Shaw DE, Shah NP, et al. Equally potent inhibition of c-Src and Abl by compounds that recognize inactive kinase conformations. Cancer Res 2009;69:2384–92.
[30] Taylor SS, Radzio-Andzelm E, Hunter T. How do protein kinases discriminate between serine/threonine and tyrosine? Structural insights from the insulin receptor protein-tyrosine kinase. FASEB J 1995;9:1255–66.
[31] Kornev AP, Haste NM, Taylor SS, Eyck LF. Surface comparison of active and inactive protein kinases identifies a conserved activation mechanism. Proc Natl Acad Sci USA 2006;103:17783–8.
[32] Tice DA, Biscardi JS, Nickles AL, Parsons SJ. Mechanism of biological synergy between cellular Src and epidermal growth factor receptor. Proc Natl Acad Sci USA 1999;96:1415–20.
[33] Taylor SS, Keshwani MM, Steichen JM, Kornev AP. Evolution of the eukaryotic protein kinases as dynamic molecular switches. Philos Trans R Soc Lond B: Biol Sci 2012;367:2517–28.
[34] Taylor SS, Kornev AP. Protein kinases: evolution of dynamic regulatory proteins. Trends Biochem Sci 2011;36:65–77.
[35] Aertgeerts K, Skene R, Yano J, Sang BC, Zou H, Snell G, et al. Structural analysis of the mechanism of inhibition and allosteric activation of the kinase domain of HER2 protein. J Biol Chem 2011;286:18756–65.
[36] Meharena HS, Chang P, Keshwani MM, Oruganty K, Nene AK, Kannan N, et al. Deciphering the structural basis of eukaryotic protein kinase regulation. PLoS Biol 2013;11(10):e1001680.

[37] Shah K, Liu Y, Deirmengian C, Shokat KM. Engineering unnatural nucleotide specificity for Rous sarcoma virus tyrosine kinase to uniquely label its direct substrates. Proc Natl Acad Sci USA 1997;94:3565–70.
[38] Liu Y, Shah K, Yang F, Witucki L, Shokat KM. A molecular gate which controls unnatural ATP analogue recognition by the tyrosine kinase v-Src. Bioorg Med Chem 1998;6:1219–26.
[39] Cauthron RD, Symcox MM, Shuntoh H. Autoactivation of catalytic (Cα) subunit of cyclic AMP-dependent protein kinase by phosphorylation of threonine 197. Mol Cell Biol 1993;13:2332–41.
[40] Steichen JM, Kuchinskas M, Keshwani MM, Yang J, Adams JA, Taylor SS. Structural basis for the regulation of protein kinase A by activation loop phosphorylation. J Biol Chem 2012;287:14672–80.
[41] Johnson DA, Akamine P, Radzio-Andzelm E, Madhusudan M, Taylor SS. Dynamics of cAMP-dependent protein kinase. Chem Rev 2001;101:2243–70.
[42] Hanks SK, Quinn AM, Hunter T. The protein kinase family: conserved features and deduced phylogeny of the catalytic domains. Science 1988;241:42–52.
[43] Songyang Z, Carraway III KL, Eck MJ, Harrison SC, Feldman RA, Mohammadi M, et al. Catalytic specificity of protein-tyrosine kinases is critical for selective signalling. Nature 1995;373:536–9.
[44] Zhou J, Adams JA. Participation of ADP dissociation in the rate-determining step in cAMP-dependent protein kinase. Biochemistry 1997;36:15733–8.
[45] Yang J, Wu J, Steichen JM, Kornev AP, Deal MS, Li S, et al. A conserved Glu–Arg salt bridge connects coevolved motifs that define the eukaryotic protein kinase fold. J Mol Biol 2012;415:666–79.
[46] Hengge AC. Mechanistic studies on enzyme-catalyzed phosphoryl transfer. Adv Phys Org Chem 2005;40:49–108.
[47] Ho M, Bramson HN, Hansen DE, Knowles JR, Kaiser ET. Stereochemical course of the phospho group transfer catalyzed by cAMP-dependent protein kinase. J Am Chem Soc 1988;110:2680–1.
[48] Guthrie RD, Jencks WP. IUPAC recommendations for the representation of reaction mechanisms. Acc Chem Res 1989;10:343–9.
[49] Schramm VL. Enzymatic transition states and transition state analog design. Annu Rev Biochem 1998;67:693–720.
[50] Schramm VL. Transition states, analogues, and drug development. ACS Chem Biol 2013;8:71–81.
[51] Valiev M, Yang J, Adams JA, Taylor SS, Weare JH. Phosphorylation reaction in cAPK protein kinase-free energy quantum mechanical/molecular mechanics simulations. J Phys Chem 2007;111:13455–64 [Erratum in: J Phys Chem 2010;114:6763].
[52] Cheng Y, Zhang Y, McCammon JA. How does the cAMP-dependent protein kinase catalyze the phosphorylation reaction: an ab initio QM/MM study. J Am Chem Soc 2005;127:1553–62.
[53] Bao ZQ, Jacobsen DM, Young MA. Briefly bound to activate: transient binding of a second catalytic magnesium activates the structure and dynamics of CDK2 kinase for catalysis. Structure 2011;19:675–90.
[54] Pauling L. Chemical achievement and hope for the future. Am Sci 1948;36:51–8.
[55] Amyes TL, Richard JP. Specificity in transition state binding: the Pauling model revisited. Biochemistry 2013;52:2021–35.
[56] De Clercq E. Strategies in the design of antiviral drugs. Nat Rev Drug Discov 2002;1:13–25.
[57] Roberts NA, Martin JA, Kinchington D, Broadhurst AV, Craig JC, Duncan IB, et al. Rational design of peptide-based HIV proteinase inhibitors. Science 1990;248:358–61.
[58] De Clercq E. Antivirals: past, present and future. Biochem Pharmacol 2013;85:727–44.
[59] Armstrong RN, Kondo H, Granot J, Kaiser ET, Mildvan AS. Magnetic resonance and kinetic studies of the manganese(II) ion and substrate complexes of the catalytic subunit of adenosine 3′,5′-monophosphate dependent protein kinase from bovine heart. Biochemistry 1979;18:1230–8.
[60] Cook PF, Neville Jr ME, Vrana KE, Hartl FT, Roskoski Jr R. Adenosine cyclic 3′,5′-monophosphate dependent protein kinase: kinetic mechanism for the bovine skeletal muscle catalytic subunit. Biochemistry 1982;21:5794–9.
[61] Jacobsen DM, Bao ZQ, O'Brien P, Brooks 3rd CL, Young MA. Price to be paid for two-metal catalysis: magnesium ions that accelerate chemistry unavoidably limit product release from a protein kinase. J Am Chem Soc 2012;134:15357–70.
[62] Liu M, Girma E, Glicksman MA, Stein RL. Kinetic mechanistic studies of Cdk5/p25-catalyzed H1P phosphorylation: metal effect and solvent kinetic isotope effect. Biochemistry 2010;49:4921–9.
[63] Waas WF, Dalby KN. Physiological concentrations of divalent magnesium ion activate the serine/threonine specific protein kinase ERK2. Biochemistry 2003;42:2960–70.
[64] Sun G, Budde RJ. Requirement for an additional divalent metal cation to activate protein tyrosine kinases. Biochemistry 1997;36:2139–46.
[65] Vicario PP, Saperstein R, Bennun A. Role of divalent metals in the kinetic mechanism of insulin receptor tyrosine kinase. Arch Biochem Biophys 1988;261:336–45.
[66] Wang C, Hirai TJ, Adams JA. A second magnesium ion is critical for ATP binding in the kinase domain of the oncoprotein v-Fps. Biochemistry 1998;37:12624–30.
[67] Fersht A. Enzyme structure and mechanism. 2nd ed. New York: W.H. Freeman and Company; 1985. p. 105–6.
[68] Mukherjee K, Sharma M, Urlaub H, Bourenkov GP, Jahn R, Südhof TC, et al. CASK Functions as a Mg^{2+}-independent neurexin kinase. Cell 2008;133:328–39.
[69] Gerlits O, Das A, Keshwani MM, Taylor S, Waltman MJ, Langan P, et al. Metal-free cAMP-dependent protein kinase can catalyze phosphoryl transfer. Biochemistry 2014;53:3179–86.
[70] Zheng J, Knighton DR, ten Eyck LF, Karlsson R, Xuong N, Taylor SS, et al. Crystal structure of the catalytic subunit of cAMP-dependent protein kinase complexed with MgATP and peptide inhibitor. Biochemistry 1993;32:2154–61.
[71] Adams JA, Taylor SS. Divalent metal ions influence catalysis and active-site accessibility in the cAMP-dependent protein kinase. Protein Sci 1993;2:2177–86.
[72] Adams JA. Kinetic and catalytic mechanisms of protein kinases. Chem Rev 2001;101:2271–90.
[73] Bastidas AC, Deal MS, Steichen JM, Guo Y, Wu J, Taylor SS. Phosphoryl transfer by protein kinase A is captured in a crystal lattice. J Am Chem Soc 2013;135:4788–98.
[74] Peng YH, Shiao HY, Tu CH, Liu PM, Hsu JT, Amancha PK, et al. Protein kinase inhibitor design by targeting the Asp–Phe–Gly (DFG) motif: the role of the DFG motif in the design of epidermal growth factor receptor inhibitors. J Med Chem 2013;56:3889–903.
[75] Herbst RS, Heymach JV, Lippman SM. Lung cancer. N Engl J Med 2008;359:1367–80.
[76] Lynch TJ, Bell DW, Sordella R, Gurubhagavatula S, Okimoto RA, Brannigan BW, et al. Activating mutations in the epidermal growth factor receptor underlying responsiveness of non-small-cell lung cancer to gefitinib. N Engl J Med 2004;350:2129–39.
[77] Paez JG, Jänne PA, Lee JC, Tracy S, Greulich H, Gabriel S, et al. *EGFR* mutations in lung cancer: correlation with clinical response to gefitinib therapy. Science 2004;304:1497–500.
[78] Pao W, Miller V, Zakowski M, Doherty J, Politi K, Sarkaria I, et al. EGF receptor gene mutations are common in lung cancers from "never smokers" and are associated with sensitivity of tumors to gefitinib and erlotinib. Proc Natl Acad Sci USA 2004;101:13306–11.
[79] Massarelli E, Johnson FM, Erickson HS, Wistuba II, Papadimitrakopoulou V. Uncommon epidermal growth factor receptor mutations in non-small cell lung cancer and their mechanisms of EGFR tyrosine kinase inhibitors sensitivity and resistance. Lung Cancer 2013;80:235–41.
[80] Cohen MH, Williams GA, Sridhara R, Chen G, McGuinn Jr WD, Morse D, et al. United States Food and Drug Administration Drug Approval summary: Gefitinib (ZD1839; Iressa) tablets. Clin Cancer Res 2004;10:1212–8.
[81] Cohen MH, Johnson JR, Chen YF, Sridhara R, Pazdur R. FDA drug approval summary: erlotinib (Tarceva) tablets. Oncologist 2005;10:461–6.
[82] Yun CH, Boggon TJ, Li Y, Woo MS, Greulich H, Meyerson M, et al. Structures of lung cancer-derived EGFR mutants and inhibitor complexes: mechanism of activation and insights into differential inhibitor sensitivity. Cancer Cell 2007;11:217–27.
[83] Red Brewer M, Yun CH, Lai D, Lemmon MA, Eck MJ, Pao W. Mechanism for activation of mutated epidermal growth factor receptors in lung cancer. Proc Natl Acad Sci USA 2013;110:E3595–604 [Erratum in: Proc Natl Acad Sci USA 2013;110(50):20344].
[84] Ryan Q, Ibrahim A, Cohen MH, Johnson J, Ko CW, Sridhara R, et al. FDA drug approval summary: lapatinib in combination with capecitabine for previously treated metastatic breast cancer that overexpresses HER-2. Oncologist 2008;13:1114–9.
[85] Paz-Ares L, Soulières D, Melezínek I, Moecks J, Keil L, Mok T, et al. Clinical outcomes in non-small-cell lung cancer patients with EGFR mutations: pooled analysis. J Cell Mol Med 2010;14:51–69.
[86] Sequist LV, Waltman BA, Dias-Santagata D, Digumarthy S, Turke AB, Fidias P, et al. Genotypic and histological evolution of lung cancers acquiring resistance to EGFR inhibitors. Sci Transl Med 2011;3:75ra26.
[87] Solca F, Dahl G, Zoephel A, Bader G, Sanderson M, Klein C, et al. Target binding properties and cellular activity of afatinib (BIBW 2992), an irreversible ErbB family blocker. J Pharmacol Exp Ther 2012;343:342–50.
[88] Yun CH, Mengwasser KE, Toms AV, Woo MS, Greulich H, Wong KK, et al. The T790 M mutation in EGFR kinase causes drug resistance by increasing the affinity for ATP. Proc Natl Acad Sci USA 2008;105:2070–5.
[89] Roskoski Jr R. Anaplastic lymphoma kinase (ALK): structure, oncogenic activation, and pharmacological inhibition. Pharmacol Res 2013;68:68–94.
[90] Engelman JA, Zejnullahu K, Mitsudomi T, Song Y, Hyland C, Park JO, et al. *MET* amplification leads to gefitinib resistance in lung cancer by activating ERBB3 signaling. Science 2007;316:1039–43.
[91] Carmi C, Mor M, Petronini PG, Alfieri RR. Clinical perspectives for irreversible tyrosine kinase inhibitors in cancer. Biochem Pharmacol 2012;84:1388–99.
[92] Roskoski Jr R. The preclinical profile of crizotinib for the treatment of non-small-cell lung cancer and other neoplastic disorders. Expert Opin Drug Discov 2013;8:1165–79.
[93] Dungo RT, Keating GM. Afatinib: first global approval. Drugs 2013;73:1503–15.
[94] Cataldo VD, Gibbons DL, Pérez-Soler R, Quintás-Cardama A. Treatment of non-small-cell lung cancer with erlotinib or gefitinib. N Engl J Med 2011;364:947–55.
[95] Geyer CE, Forster J, Lindquist D, Chan S, Romieu CG, Pienkowski T, et al. Lapatinib plus capecitabine for HER2-positive advanced breast cancer. N Engl J Med 2006;355:2733–43 [Erratum in: N Engl J Med 2007;356:1487].
[96] Riemsma R, Forbes CA, Amonkar MM, Lykopoulos K, Diaz JR, Kleijnen J, et al. Systematic review of lapatinib in combination with letrozole compared with other first-line treatments for hormone receptor positive (HR+)

and HER2+ advanced or metastatic breast cancer (MBC). Curr Med Res Opin 2012;28:1263–79.
[97] Soria JC, Cortes J, Massard C, Armand JP, De Andreis D, Ropert S, et al. Phase I safety, pharmacokinetic and pharmacodynamic trial of BMS-599626 (AC480), an oral pan-HER receptor tyrosine kinase inhibitor, in patients with advanced solid tumors. Ann Oncol 2012;23:463–71.
[98] Majem M, Pallarès C. An update on molecularly targeted therapies in second- and third-line treatment in non-small cell lung cancer: focus on EGFR inhibitors and anti-angiogenic agents. Clin Transl Oncol 2013;15:343–57.
[99] Bello CL, Smith E, Ruiz-Garcia A, Ni G, Alvey C, Loi CM. A phase I, open-label, mass balance study of [^{14}C] dacomitinib (PF-00299804) in healthy male volunteers. Cancer Chemother Pharmacol 2013;72:379–85.
[100] Yu HA, Riely GJ. Second-generation epidermal growth factor receptor tyrosine kinase inhibitors in lung cancers. J Natl Compr Cancer Netw 2013;11:161–9.
[101] Jørgensen JT. Role of human epidermal growth factor receptor 2 in gastric cancer: biological and pharmacological aspects. World J Gastroenterol 2014;20:4526–35.
[102] Dorsey K, Agulnik M. Promising new molecular targeted therapies in head and neck cancer. Drugs 2013;73:315–25.
[103] Yang G, Yao Y, Zhou J, Zhao Q. Effects of icotinib, a novel epidermal growth factor receptor tyrosine kinase inhibitor, in EGFR-mutated non-small cell lung cancer. Oncol Rep 2012;27:2066–72.
[104] Cohen RB. Current challenges and clinical investigations of epidermal growth factor receptor (EGFR)- and ErbB family-targeted agents in the treatment of head and neck squamous cell carcinoma (HNSCC). Cancer Treat Rev 2013. S0305-7372(13)00206-5.
[105] Zhao Q, Shentu J, Xu N, Zhou J, Yang G, Yao Y, et al. Phase I study of icotinib hydrochloride (BPI-2009H), an oral EGFR tyrosine kinase inhibitor, in patients with advanced NSCLC and other solid tumors. Lung Cancer 2011;73:195–202.
[106] Liang W, Wu X, Fang W, Zhao Y, Yang Y, Hu Z, et al. Network meta-analysis of erlotinib, gefitinib, afatinib and icotinib in patients with advanced non-small-cell lung cancer harboring EGFR mutations. PLoS ONE 2014;9:e5 8524.
[107] Martin M, Martin M, Geyer Jr CE, Ito Y, Ro J, Lang I, et al. A phase two randomised trial of neratinib monotherapy versus lapatinib plus capecitabine combination therapy in patients with HER2+ advanced breast cancer. Eur J Cancer 2013;49:3763–72.
[108] Gandhi L, Bahleda R, Tolaney SM, Kwak EL, Cleary JM, Pandya SS, et al. Phase I study of neratinib in combination with temsirolimus in patients with human epidermal growth factor receptor 2-dependent and other solid tumors. J Clin Oncol 2014;32:68–75.
[109] Kim HJ, Kim HP, Yoon YK, Kim MS, Lee GS, Han SW, et al. Antitumor activity of HM781-36B, a pan-HER tyrosine kinase inhibitor, in HER2-amplified breast cancer cells. Anticancer Drugs 2012;23:288–97.
[110] Cha MY, Lee KO, Kim M, Song JY, Lee KH, Park J, et al. Antitumor activity of HM781-36B, a highly effective pan-HER inhibitor in erlotinib-resistant NSCLC and other EGFR-dependent cancer models. Int J Cancer 2012;130:2445–54.
[111] Nam HJ, Kim HP, Yoon YK, Hur HS, Song SH, Kim MS, et al. Antitumor activity of HM781-36B, an irreversible Pan-HER inhibitor, alone or in combination with cytotoxic chemotherapeutic agents in gastric cancer. Cancer Lett 2011;302:155–65.
[112] Doi T, Takiuchi H, Ohtsu A, Fuse N, Goto M, Yoshida M, et al. Phase I first-in-human study of TAK-285, a novel investigational dual HER2/EGFR inhibitor, in cancer patients. Br J Cancer 2012;106:666–72.
[113] Lorusso P, Venkatakrishnan K, Chiorean EG, Noe D, Wu JT, Sankoh S, et al. Phase 1 dose-escalation, pharmacokinetic, and cerebrospinal fluid distribution study of TAK-285, an investigational inhibitor of EGFR and HER2. Invest New Drugs 2014;32:160–70.
[114] Sim MW, Cohen MS. The discovery and development of vandetanib for the treatment of thyroid cancer. Expert Opin Drug Discov 2014;9:105–14.
[115] Sakuma Y, Yamazaki Y, Nakamura Y, Yoshihara M, Matsukuma S, Nakayama H, et al. WZ4002, a third-generation EGFR inhibitor, can overcome anoikis resistance in EGFR-mutant lung adenocarcinomas more efficiently than Src inhibitors. Lab Invest 2012;92:371–83.
[116] Sánchez-Martín M, Pandiella A. Differential action of small molecule HER kinase inhibitors on receptor heterodimerization: therapeutic implications. Int J Cancer 2012;131:244–52.